Graduate Theses and Dissertations   Graduate School

January 2013

Time Scale of Groundwater Recharge: A Generalized Modeling Technique

Makhan Virdi
University of South Florida, mlvirdi@gmail.com

Follow this and additional works at: http://scholarcommons.usf.edu/etd

Part of the Civil Engineering Commons, and the Water Resource Management Commons

Time Scale of Groundwater Recharge: A Generalized Modeling Technique

by

Makhan Virdi

A dissertation submitted in partial fulfillment
of the requirements for the degree of
Doctor of Philosophy
Department of Civil and Environmental Engineering
College of Engineering
University of South Florida

Major Professor: Mark Ross, Ph.D.
Mark Stewart, Ph.D.
Kenneth Trout, Ph.D.
Aydin Sunol, Ph.D.
Terrie Lee, M.E.

Date of Approval:
July 3, 2013

Keywords: wetting front, arrival time, wet equilibrium, recharge progression, water table

Dedication

To my parents, who instilled in me a passion for learning. Thank you, *ammi* and *daddy*, for showing me the importance and power of dreaming big.

"Ricordati, quando commenti l'acque, d'allegar prima la sperienza e poi la ragione"

[Remember, when discoursing on water, to adduce first experience and then reason]

– *Leonardo da Vinci*

Acknowledgments

I am grateful to my parents for their constant love, support and encouragement. They always knew the value of education and worked tirelessly to provide me with the necessary means and modes to make sure that I receive the best education. They have always inspired me to keep an open mind, reason, challenge conformity, and question existing dogma. Thank you, *mom* and *dad*, for everything you are, do, and have done.

My family has been a source of inspiration and encouragement throughout my life. Reena and Nisha, thank you for being the most adorable sisters. Kuldip, you are definitely the best brother anyone can ask for and I have deepest regards for you as a person and as a friend. I would like to thank my elder sister Sumitra, and Dr. Balvir for their support.

I am extremely thankful to Dr. Mark Ross for his support and encouragement through all the years at the University of South Florida. I am thankful to Terrie Lee for being a motivating force. I want to thank my doctoral committee members for their input and overall assistance in completing this dissertation.I would like to thank Dr. Ken Trout for always being available for guidance. I am grateful to Dr. Manoj Arora (Director, PEC University of Technology, Chandigarh, India) for being an excellent mentor since my undergraduate years at IIT Roorkee.

I would like to thank my colleagues at the Center for Modeling Hydrologic and Aquatic Systems (*CMHAS*) for their input and assistance with my research. I would like to thank my friends who are always available for any kind of help. I can not mention each one of you here but I want to convey that I value your friendship.

Finally, I would like to express my appreciation for the spirit of free and open source software and tools that inspire me to contribute back to the community.

Table of Contents

List of Tables

List of Figures

Abstract

Estimating the quantity of water that reaches the water table following an infiltration event is vital for modeling and management of water resources. Estimating the time scale of groundwater recharge after a rainfall event is difficult because of the dependence on nonlinear soil characteristics and variability in antecedent conditions. Modeling the flow of water through the variably saturated zone is computationally intensive since it requires simulation of Richards' equation, a nonlinear partial differential equation without a closed-form analytical solution, with parametric relationships that are difficult to approximate. Hence, regional scale coupled (surface water - groundwater) hydrological models make simplistic assumptions about the quantity and timing of recharge following infiltration. For simplicity, such models assume the quantity of recharge to be a fraction of the total rainfall and the time to recharge the saturated groundwater is scaled proportionally to the depth to water table, in lieu of simulating computationally intensive flow in the variably saturated zone. In integrated or coupled (surface water - groundwater) regional scale hydrological models, better representation of the timing and quantity of groundwater recharge is required and important for water resources management. This dissertation presents a practical groundwater recharge estimation method and relationships that predict the timing and volume accumulation of groundwater recharge to moderate to deep water table settings.

This study combines theoretical, empirical, and simulation techniques to develop a relatively simple model to estimate the propagation of the soil moisture wetting front through variably saturated soil. This model estimates the time scale and progression of recharge following infiltration for a specified depth to water table, saturated hydraulic conductivity and equilibrium moisture condition. High-resolution soil moisture data from

a set of experiments conducted in a laboratory soil column were used to calibrate the HYDRUS-1D model.

The calibrated model was used to analyze the time scale of recharge by varying soil hydraulic properties and simulating the application of rainfall pulses of varying volume and intensities. Modeling results were used to develop an equation that relates the non-dimensional travel time of the wetting front to excess moisture content above equilibrium. This research indicates that for a soil with a known retention curve, the wetting front arrival time at a given depth can be described by a power law, where the power is a function of the saturated hydraulic conductivity. This equation relates the non-dimensional travel time of the wetting front to excess moisture content above a defined *'wet' equilibrium* moisture content. Even though the equilibrium moisture content is dependent on the soil water retention characteristics, the powers in the equation governing the timing of recharge depend mostly on the saturated hydraulic conductivity for a little variation in water retention curve. Also, the power law relates recharge (normalized by applied pulse volume) to time (normalized by the time of arrival of wetting front at that depth). The resulting equations predicted the model simulated normalized (relative) recharge with root mean square errors of less than 14 percent for the tested cases.

Chapter 1   Introduction

1.1   Background

Predicting the timing and volume of groundwater recharge following infiltration is important for groundwater modeling investigations and estimating water budgets, quantifying and managing water resources because the infiltration volume progresses through an evapotranspiration uptake horizon (root zone). Recharge is an ongoing process and different aspects of the process occur over a range of time scales, from minutes to weeks. One important aspect of recharge is the time required for a wetting front from a distinct rainfall event to arrive at the water table. Time scale of recharge can be defined as the time taken by the wetting front to get from the soil surface to the water table at a certain depth in the surficial aquifer. The estimation of the time scale of recharge has become more important for the coupled and integrated surface water-groundwater models. The challenges for modeling arise from the complex interactions between the saturated and unsaturated zones. Various techniques exist to estimate the time scale of recharge (travel time) and the quantity of recharge with varying degrees of reliability and simplicity [Richards et al., 2005; Scanlon et al., 2002]. For instance, the water table fluctuation (WTF) method uses the fluctuations in water table and the specific yield to estimate recharge [Gerhart, 1986; Hall and Risser, 1993]. The timing and quantity of groundwater recharge remains poorly understood because of the non-linear nature of the unsaturated zone processes, a lack of available soil parameters, and the numerical and computational complexity of modeling these processes. It is important to account for water balance at regional scales to address environmental and water management concerns [Hughes and Liu, 2008]. Unsaturated zone

processes are often approximated or ignored in groundwater models because of the relative complexity of modeling because of the variety of soil types and associated soil hydraulic properties. In general, the variably saturated zone processes are poorly understood and is a field of active research [Harter and Hopmans, 2004].

1.2 Motivation

The travel time of the wetting front (time scale of recharge) affects the amount of water available for root water uptake after a rainfall event as it passes through the root zone. Groundwater models use recharge flux as a top boundary condition. For simplicity, many groundwater models use a fraction of the applied rainfall as recharge for the top boundary condition. For soils in Florida ridge settings, the recharge to groundwater was found to be in the range of 43 to 53 percent of the annual rainfall for water table shallower than 10 ft [Sumner, 1996]. The timing of recharge for some models is calculated by lagging the recharge by the time proportional to the depth to the water table [Swancar and Lee, 2003]. A variation of this method ignores rainfall events below a 'threshold' and also assumes the recharge to be zero for events less than the daily evaporation [Lee, 1996]. A study by Virdi et al. [2012] used a model based on kinematic-wave approximation of variably saturated flow combined with existing fully saturated groundwater models to simulate surface-groundwater interactions. Several integrated groundwater-surface water models exist with capabilities to model groundwater recharge through the unsaturated zone, *e.g.*, MIKE SHE, IHM (Integrated Hydrologic Model) and GSFLOW [DHI, 2004; Markstrom et al., 2008; Ross et al., 2004]. MIKE SHE is a commercially available fully coupled model to simulate saturated-unsaturated groundwater flow which has been tested and reviewed in literature [Graham and Butts, 2005; Hughes and Liu, 2008; Illangasekare and Prucha, 2001]. In MIKE SHE, unsaturated zone flow can be simulated using the following 3 options:

- *1-D form of Richards' Equation Approach:* A fully implicit finite-difference solution for 1-D unsaturated zone model for each grid element. It requires the full specifica-

tion of the moisture retention curve and the unsaturated conductivity relation. It is computationally intensive and is prone to numerical instabilities and convergence issues [DHI, 2004].

- *Gravity Flow Approach:* This approach involves explicit finite-difference gravity drainage solution in 1-D for each grid. It ignores capillary effects, and assumes a uniform vertical gradient entirely due to gravity (only gravity head). It requires the unsaturated conductivity relation to be specified but no water retention curve is required. This approach uses the finite element method to solve the continuity equation from top of the column to the water table; adding the bottom flux to the saturated zone. It is unconditionally stable, faster than solving the Richards' equation, and used when delayed recharge to groundwater table is needed. However, this method is overly simplistic and does not capture the unsaturated zone suction head contribution.

- *Two-Layer Water Balance Approach:* This approach uses linear water balance approach with uniform soil for the entire depth of the grid soil column, divided into root zone and another zone that extends from root zone to the water table. This approach is generally good for shallow water table environments.

In general, the solution of Richards' equation can be used to estimate timing and magnitude of recharge but it is computationally very expensive and unstable even if it is solved in its one dimensional form. It requires a lot of soil hydraulic properties which may be expensive and time consuming to obtain in the field or laboratory.

The research question addressed by this dissertation is:

"How can we simplify the representation and quantification of the timing and volume accumulation of groundwater recharge in coupled hydrological models using easily obtainable soil hydraulic parameters?"

The dissertation focuses on developing a generalized model for time scale of groundwater recharge using simple parameters like depth to water table, vertical saturated hydraulic conductivity and rainfall volume. This study is based on data generated from model simulations and a set of experiments on a 2 meter tall laboratory soil column and analyzing the corresponding high spatio-temporal resolution soil moisture data for timing and quantity of recharge.

1.3 Contribution

This dissertation provides a framework for better representation of groundwater recharge process in coupled and integrated hydrological models. The proposed models are simple, computationally inexpensive and require a few, easily obtainable soil hydraulic parameters. This approach should be useful for representing and calculating groundwater recharge when the soil data available for modeling groundwater recharge is limited. Furthermore, the method is relatively accurate for groundwater recharge and provides a simple alternative to numerically unstable non-linear equations representing the flow in the unsaturated zone.

This study contributes to improve current understanding of the timing and quantity of groundwater recharge (Figure 1.1). These insights can be employed to better represent the recharge processes in groundwater-surface water coupled hydrological models. To study the time scale of recharge, a robust automated framework was developed to run HYDRUS-1D simulations over rigorous sets of combinations of soil hydraulic parameters and applied rainfall volumes. This framework generates sets of input files for simulation and saves output files for visualization and analysis for developing the proposed models. A rigorous analysis of simulated data was used to propose models to (a) predict time scale of recharge at a given depth based on the arrival time of the wetting front, and (b) predict the progression of recharge over time at the given depth.
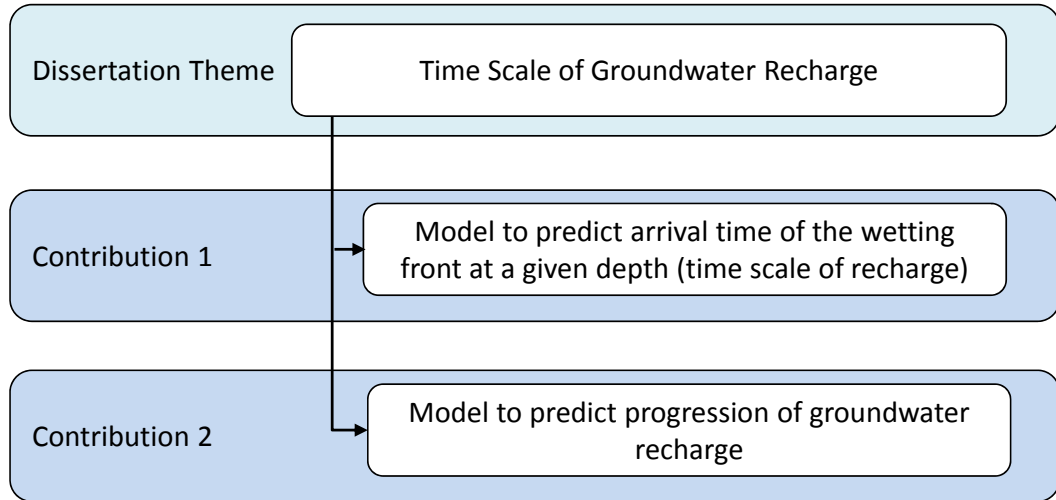
Figure 1.1: Contributions of this dissertation. A brief description is provided in Section 1.3

Here is a brief description of the contributions described in this dissertation:

- *Model to predict arrival time of the wetting front at a given depth (time scale of recharge):* A power law model was proposed to predict the time scale of recharge at a given depth based on the saturated hydraulic conductivity of the soil. This model is independent of the applied rainfall pulse volume and intensity for soils with moisture above the 'wet' equilibrium.

- *Model to predict progression of groundwater recharge:* After the onset of recharge is predicted by the aforementioned model, the progression of the recharge (relative to the total rainfall pulse volume) over time can be predicted by this model.

1.4 Outline

This dissertation is organized into a total of 5 chapters and 4 appendices. Chapter 2 describes the data and materials used in this study. Chapter 3 described the methodology used to develop the models proposed in this dissertation. This chapter discussed the theoretical background, model simulations and the analysis of the data to develop the

proposed models for estimating the timing and quantity of recharge. The discussion of results of model development and validation of the proposed models is provided in Chapter 4. Finally, Chapter 5 summarizes the proposed models and the methods used in this study and concludes the findings of this dissertation. The terms used in this manuscript are defined in Appendix A. The notations used are listed in Appendix B. The computer programs developed to analyze the data are provided in Appendix C and Appendix D.

Chapter 2 Data and Methodology

2.1 Introduction

This study utilizes data from field instrumentation, a laboratory soil column under controlled conditions, and computer model simulations. The high resolution soil moisture data and water table data from the field instrumentation were used to study the propagation of the wetting front following a rainfall event. These data were also used to estimate water budget components like evapotranspiration, runoff, infiltration, *etc.* [CMHAS, 2011; Rahgozar et al., 2007, 2012; Rahgozar, 2006]. The laboratory soil column was constructed to mimic the composition of soil from the field study area. This soil column was used to study the recharge processes in controlled conditions with the absence of evapotranspiration. The high resolution observed data from the soil column were used to calibrate a HYDRUS-1D model [Šimůnek et al., 2005]. The calibrated HYDRUS-1D model was then used to run simulations with a variety of rainfall fluxes and soil properties. The simulation data from HYDRUS-1D were analyzed to find a methodology to predict the onset of recharge and progression of recharge over time.

2.2 Field Study

The ecological preserve area (ECO area) managed by the University of South Florida was used for field study. The objective of this data collection and investigation was to study the detailed water budget components including groundwater recharge, evapotranspiration (ET), runoff in a ridge type environment. The water table depth ranged from shallow (0-2

Figure 2.1: Aerial image showing the location of soil moisture monitoring sites. Transect along the hillslope is shown in Figure 2.2.

m) to more than 6 m at different locations along the hillslope transect. The data collected from this site was used to analyze the propagation of wetting fronts through the unsaturated zone. Six locations (ECO-1 through ECO-6) were identified along the transect to install soil moisture sensors and water table observation wells (Figure 2.1).

2.2.1   Instrumentation and Data Collection

Eight soil moisture sensors were installed to monitor soil moisture at 10-minutes intervals for depths ranging from 10 cm to 190 cm below land surface. Sensors were located at 10, 20, 30, 50, 80, 110, 150, and 190 cm below land surface for monitoring a 2 m deep soil column at each of the six ECO sites shown on Figure 2.2. Water table elevation at these locations was also recorded at 10-minute interval for the surficial aquifer, verified periodically using manual measurements. ECO-1 is located at the top of a sand hill and
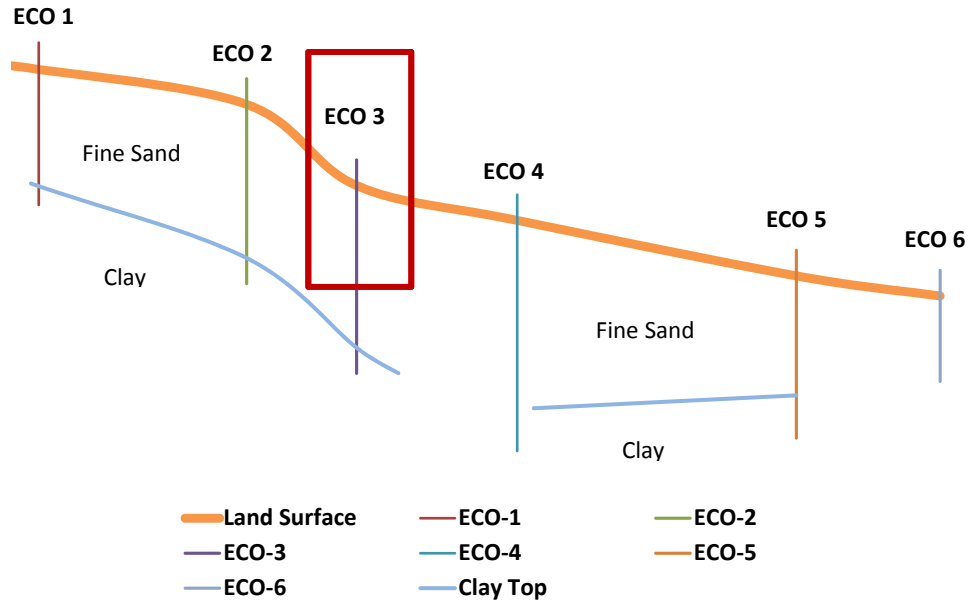
Figure 2.2: Transect along the hillslope at the ECO study area showing the location of soil moisture monitoring sites. Conceptual drawing adapted from CMHAS [2011] (not to scale).

ECO-6 is in a shallow water table environment. A weather station was also installed to monitor rainfall, wind, solar radiation and evaporation from a pan [CMHAS, 2011].

2.2.2 Recharge Analysis

The soil moisture data from the field site were analyzed along with the water table fluctuations to determine the time it takes for the wetting front to reach the water table after a rainfall event. Isolated rainfall events (with no preceding or following events in close temporal proximity) were identified to make sure that the wetting front was the result of a single event. The time of propagation for wetting front movement down through the soil column at the ECO area for two rainfall events was calculated from ECO-3 soil moisture data, water table elevation and rainfall recorded at 10-minute intervals.

The observed soil moisture data for the selected rainfall events were analyzed to determine the head and centroid of the wetting front:
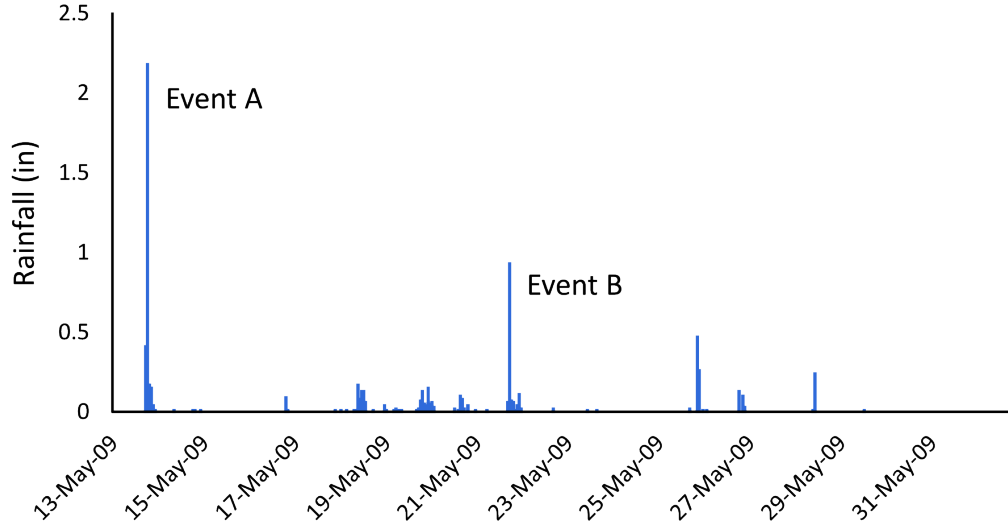
Figure 2.3: Two isolated events with relatively dry and wet Antecedent Moisture Conditions at ECO-3. Event A (dry) and Event B (wet) show the variability in initial moisture conditions.

Event A: Dry Antecedent Moisture Condition (5/13/2009)

- Propagation of the head of wetting front

- Propagation of the centroid of wetting front

Event B: Wet Antecedent Moisture Condition (5/21/2009)

- Propagation of the head of wetting front

- Propagation of the centroid of wetting front

The two selected rainfall events had different antecedent moisture conditions (AMC). The soil moisture conditions were considered relatively dry for the first event (Event A), on 5/13/2009, because no significant rainfall events took place during the preceding four weeks. The antecedent moisture conditions were relatively wet during the second rainfall event (Event B, 5/21/2009), which occurred one week after Event A (Figure 2.3) [CMHAS, 2011].

10
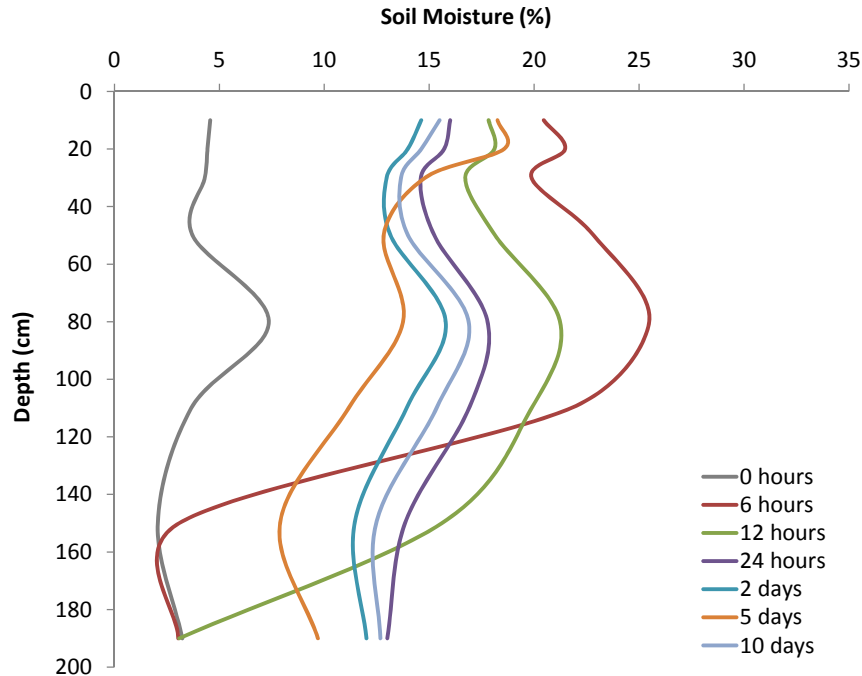
Figure 2.4: Soil Moisture profiles for dry conditions showing wetting front propagation through a 2 meter soil column following a rainfall at ECO-3. Rainfall event A: Dry AMC.

The wetting front propagation and the soil moisture distribution for Event A (2.9 inch, Dry AMC) at ECO-3, at 6 hr, 12 hr, 24 hr, 2 days, 5 days, and 10 days following the rainfall event are shown in Figure 2.4. Figure 2.5 shows the wetting front propagation and the moisture distribution following Event B (1.3 inch, Wet AMC) following a relatively wet period at the ECO-3 [CMHAS, 2011].

The time of arrival of the centroid of the wetting front to a depth was found to be approximately half that of time of the approaching head of the wetting front for event A (dry AMC) and event B (wet AMC) (Table 2.1 and Figure 2.6). It took more than 12 hours for the head of the wetting front to arrive at the bottom of the soil column (190 cm deep) for event A. For event B, this time was 17 hours (approximately). Event A (dry AMC) was much larger than event B (wet AMC), possibly contributing to the increased time needed for the wetting front of event B to travel through 190 cm soil column. However, it took
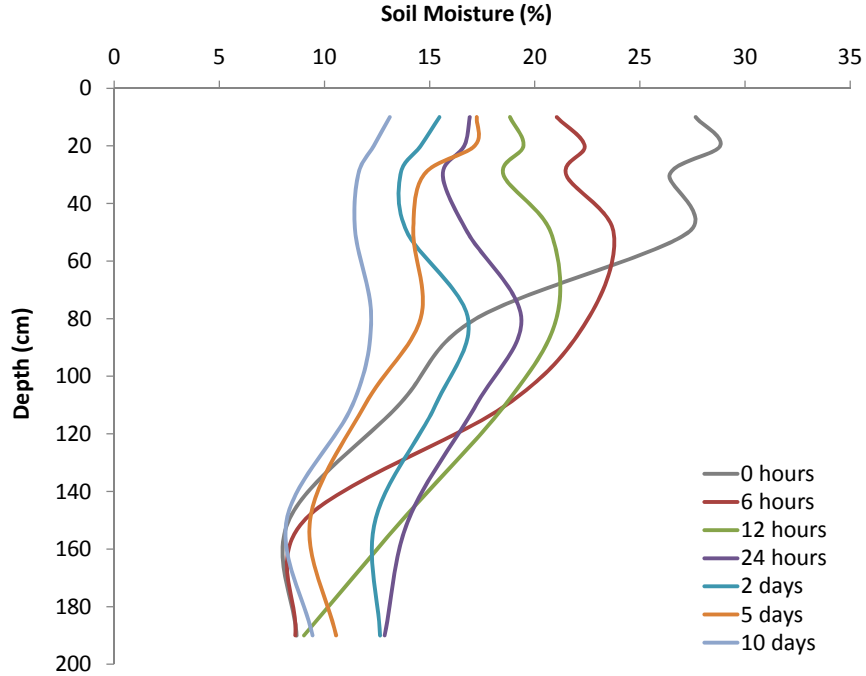
Figure 2.5: Soil Moisture profiles for wet conditions showing wetting front propagation through a 2 meter soil column following a rainfall at ECO-3. Rainfall event B: Wet AMC.

many days to several weeks for the entire pulse to reach the water table for event A and Event B [CMHAS, 2011].

Table 2.1: Time of propagation of the wetting front for two events. Events A and B corresponds to dry and wet antecedent moisture conditions.

Depth below land surface (cm)	Wetting Front (Event A)		Wetting Front (Event B)	
	Centroid timing (hr)	Head timing (hr)	Centroid timing (hr)	Head timing (hr)
10	0.7	0.33	1	0.33
20	0.75	0.5	1	0.83
30	0.83	0.67	1.17	1
50	1	0.83	1.5	1
80	2	1.33	5	1.83
110	4.17	2.5	10.33	3.33
150	10.67	5.67	18.17	8.33
190	23.83	12.17	32.33	17
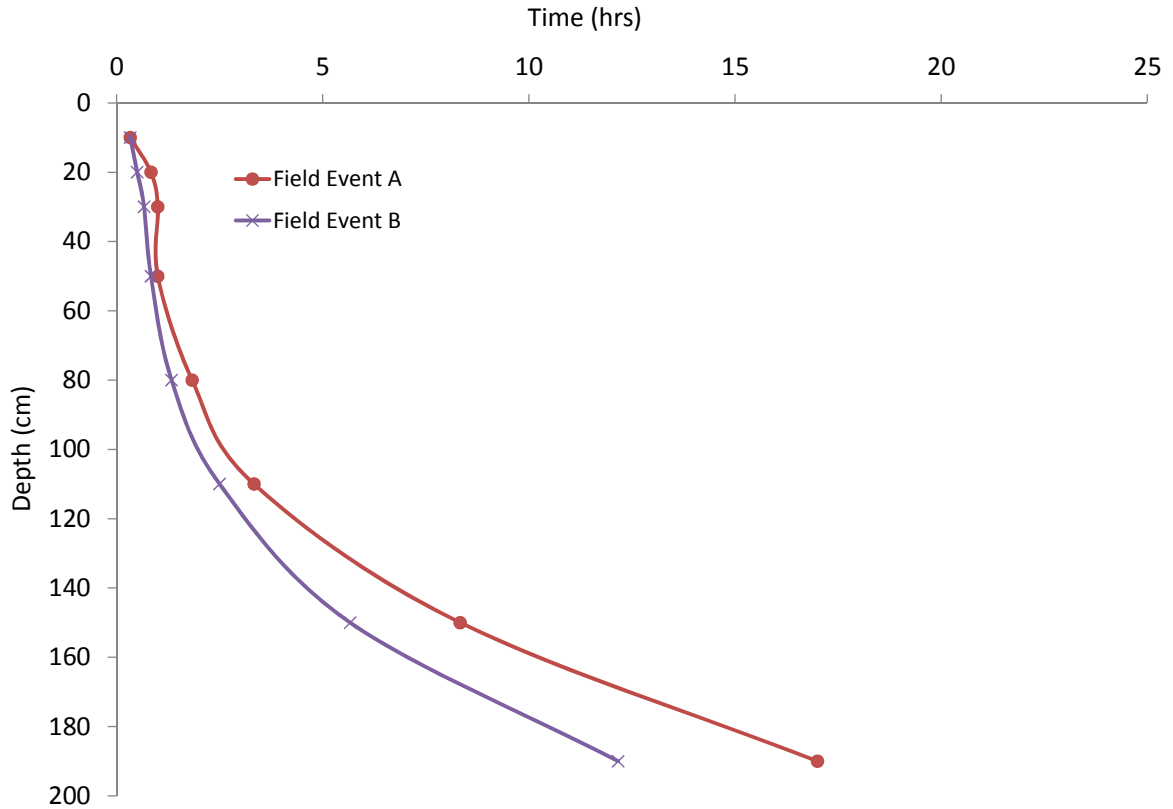
Figure 2.6: Time of propagation of wetting front for dry and wet Antecedent Moisture Conditions at ECO-3. Event A (dry) and Event B (wet) are shown.

The soil moisture data from the ECO are field study site were used to estimate the time of arrival of the wetting front at depths corresponding to depths of the soil moisture sensors. Three isolated rainfall events (with no preceding or following rainfall events) were identified to make sure that the wetting front was the result of a single event. An isolated event on July 30, 2009 was used to derive the wetting front propagation at three locations (ECO-1, ECO-3, and ECO-4). The 10-minute soil moisture data were used to determine the location and time of the wetting front corresponding to an increase in the observed soil moisture at 8 different depths. The wetting front arrival time at these depths is summarized in Table 2.2. The plot of time of arrival of the soil moisture wetting front is shown in Figure 2.7.
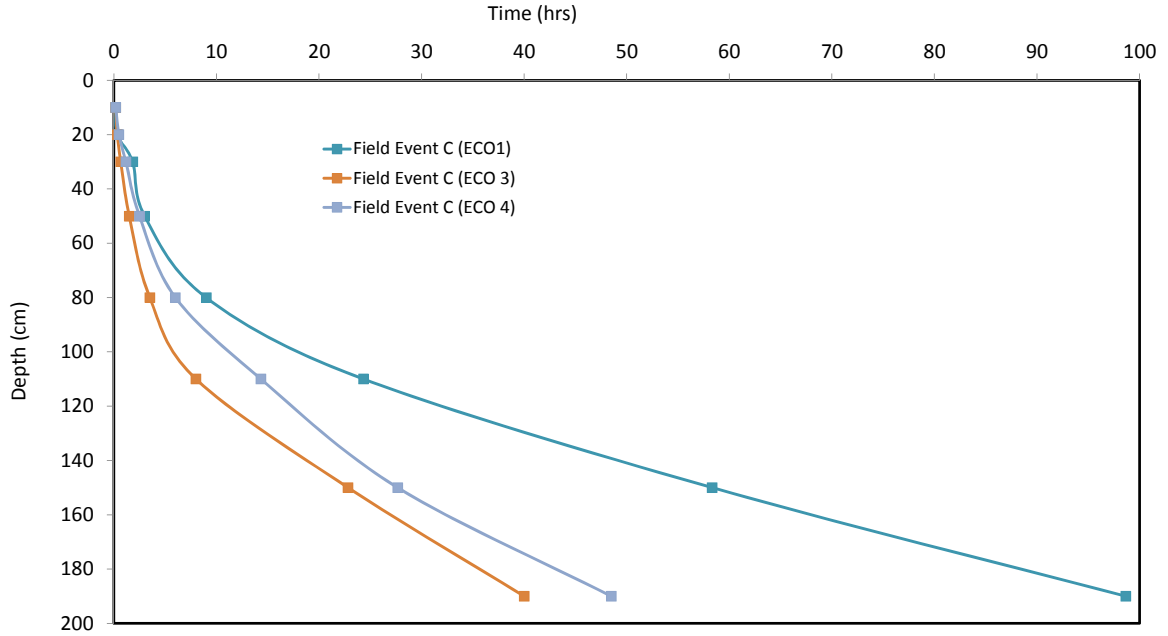
Figure 2.7: Time of arrival of the wetting front for a rainfall event at three field locations. Locations are shown in Figure 2.2.

Table 2.2: Time of arrival (hours) of the wetting front for a rainfall event at three field locations. Locations are shown in Figure 2.2.

Depth (cm)	Time of wetting front arrival (hr)		
	Location: ECO-1	Location: ECO-3	Location: ECO-4
10	0.17	0.17	0.17
20	0.33	0.33	0.50
30	1.83	0.67	1.17
50	3.00	1.50	2.50
80	9.00	3.50	6.00
110	24.33	8.00	14.33
150	58.33	22.83	27.67
190	98.67	40.00	48.50

2.3 Laboratory Soil Column

A soil column was constructed to study recharge process in controlled laboratory settings. The objective of this study was to collected high resolution soil moisture, tensiome-

ter and water table data to understand recharge timing and variability in specific yield. A three-dimensional column (square 46 cm and soil height of 160 cm) was constructed of transparent acrylic glass sheets and was open at the top and closed at the bottom and sides (Figure 2.8). The vertical soil column was filled with sand graded from 0.07 mm to 1.2 mm, with 92% of soil being less than or equal to 0.5 mm (3.5% of 20-30 graded sand, 30% of 30-65 graded sand, 17.5% of 50-140 graded sand, and 49% of 70-200 graded sand). The sand, in the soil column, was carefully compacted with a standard proctor hammer (30 blows per every 20 cm of sand) [ASTM, 2012]. After compaction the mean porosity (n) was 0.36 cc/cc. This soil is representative of the Myakka fine sand of the ECO area field study site described in Section 2.2.1.

2.3.1 Instrumentation

The laboratory setup consisted of a soil column with tensiometers, soil moisture sensors and pressure transducers. Water contents were measured using sixteen soil moisture sensors located at 8.5, 18.5, 28.5, 38.5, 48.5, 58.5, 68.5, 78.5, 88.5, 98.5, 108.5, 118.5, 128.5, 138.5, 148.5, and 158.5 cm (z=0 cm is at the soil column surface; the axis is positively downward). Water contents were measured using EnviroSCAN® soil moisture probes (available from Sentek, Adelaide, Australia) inserted into the soil column within 10 cm of each other along the soil column height [SENTEK, 2003]. Measuring the actual infiltration depth during rainfall is challenging because water content changes rapidly close to the land surface as the wetting front propagates downward. The advantage of the EnviroSCAN® technology is that multiple sensors allow for continuous monitoring of water content evolution with time from land surface to 1.5 m. At each depth listed above, the sensor provided data over a 10 cm average depth at 2-minute intervals.
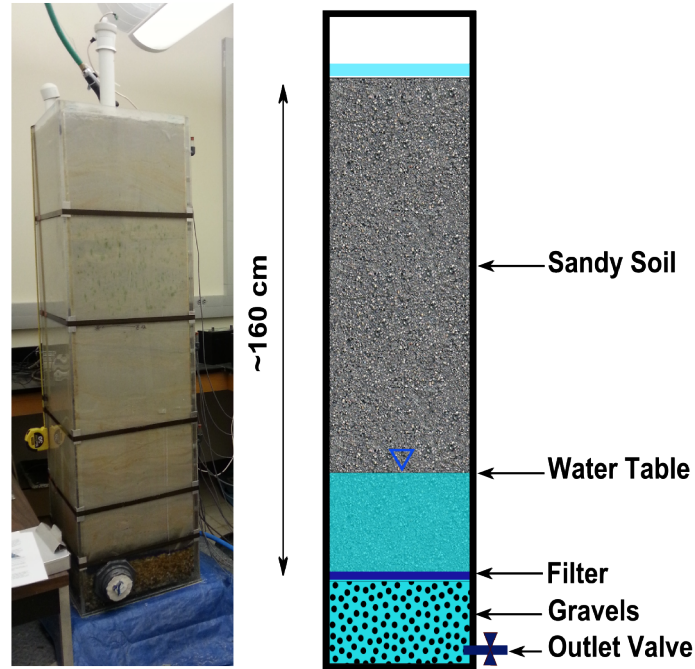
Figure 2.8: Picture and schematic of the laboratory soil column. Soil moistures sensors were installed at every 10 cm starting from the top of the column.

2.3.2 Data

Soil moisture data from the laboratory soil column was used to study wetting front propagation and calibrate HYDRUS-1D model described in Section 2.4. Soil moisture data and tension data were collected at 2-minute intervals for multiple wetting and draining events. For the draining events, the soil column was fully saturated and slowly drained to monitor the decline of water table. For the wetting event, multiple pulses (of known volume) of water were applied using a sprinkler on the top of the soil column and the progression of wetting front(s) was monitored by recording high-resolution soil moisture data, tensiometer data and water table fluctuation data.

The tensiometer data were used to fit the van Genutchen model for the water retention curve for the soil used in the laboratory soil column [van Genuchten, 1980] (Figure 2.9 and Table 2.3). These fitted values of the van Genutchen model variables were used
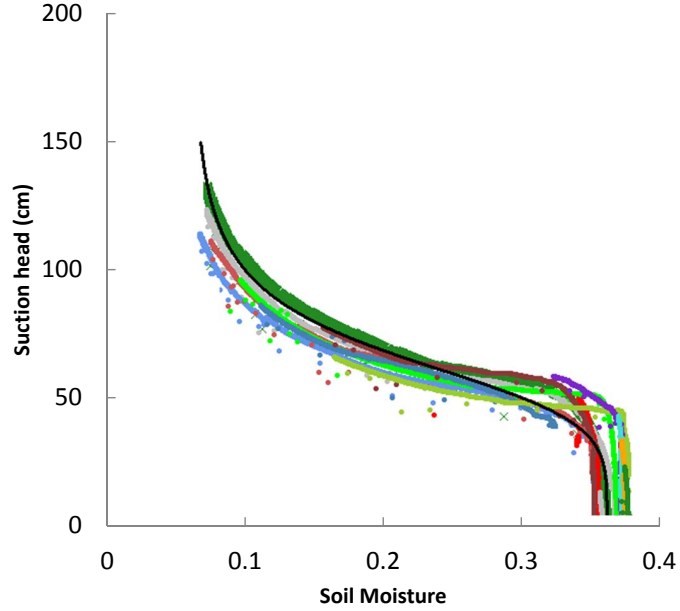
Figure 2.9: Fitted van Genutchen model (black line) to the tensiometer data observed at 10 cm depth intervals in the laboratory soil column. Different colors correspond to different depths. Fitted parameter values are given in table 2.3.

to define the soil hydrological properties for the HYDRUS-1D model representation of the soil column described in Section 2.4. Soil moisture retention curve is discussed in detail in section 3.1.1. This model was calibrated against the observed soil moisture data from the laboratory soil column.

Table 2.3: Soil hydraulic properties derived from laboratory soil column data. Values of parameters to fit van Genutchen Model (VGM) to the water retention curve.

van Genutchen Parameter	Fitted Value
θ_s	0.36
θ_r	0.045
α	0.018
N	6.378
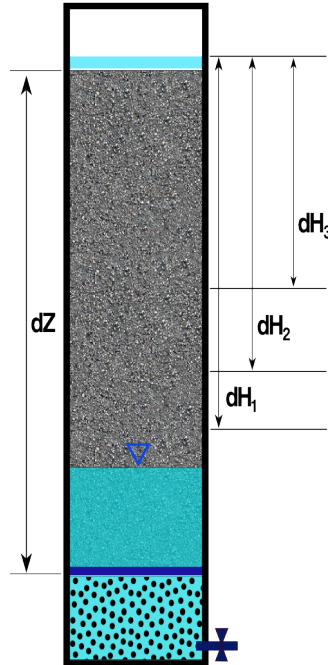
Figure 2.10: Setup used for determination of K_s in the laboratory soil column. Three different head gradients are shown.

2.3.3 Determination of Soil Hydraulic Conductivity: K_S

A constant head permeability test was done on the laboratory soil column to determine the saturated hydraulic conductivity (K_s) to be used in HYDRUS simulations. Constant head permeability tests were conducted on the soil column to measure saturated hydraulic conductivity (K_s) of the sand (Figure 2.10). Constant head permeability tests with three different head gradient (dH/dZ) conditions yielded an average value of 0.172 cm/min (8.1 ft/day) for the K_s as given in Table 2.4 and shown in Figure 2.11. This value of K_s was used to calibrate the model described in Section 2.4.

Table 2.4: Results of the constant head permeability test of the laboratory soil column. The test was conducted on three different head gradients as shown in Figure 2.11.

dH/dZ	Average q (ft/day)
0.54	4.4
0.73	6.0
0.91	7.3
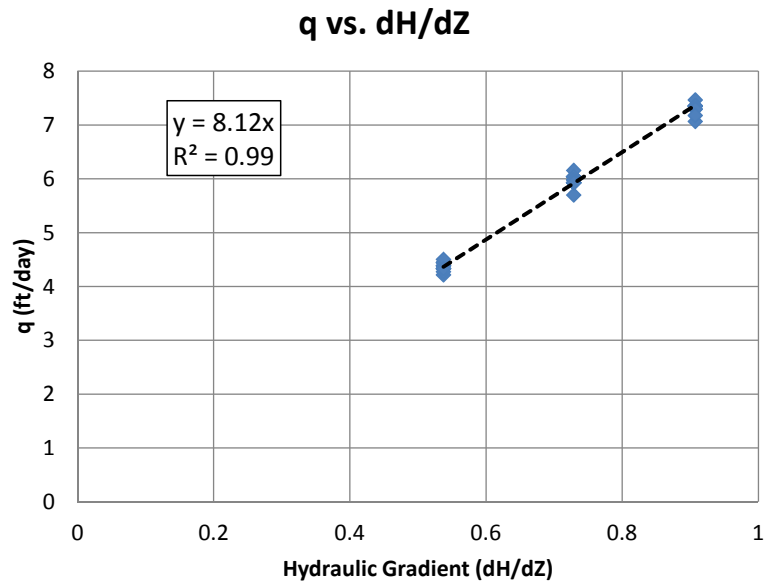
Figure 2.11: Plot of q vs dH/dZ for determination of K_s of the laboratory soil column. The slope of this curve gives the value of K_s.

2.4   HYDRUS Simulations

HYDRUS has been used extensively in research community and it has been found to reliably represent flow in the variably saturated region and simulate soil moisture [Diodato, 2000; Hernandez et al., 2003; Šimůnek et al., 2005]. A HYDRUS-1D model was set up to represent the dimensions and boundary conditions of the laboratory soil column. The objective of these model simulations was to generate data for varying conditions of applied rainfall and soil properties, and analyze that data to develop simple models to estimate groundwater recharge timing and quantity.

2.4.1   Model Set Up

A 160 cm vertical soil column was set up as a HYDRUS-1D model representing the laboratory soil column. Observation points were set up at 16 locations corresponding to the location of the soil moisture sensors and tensiometer sensors in the laboratory column. The model simulations cover a period of 100 days with time-steps (with a maximum of 2 minutes) to match the 2-minute temporal resolution of the data collected from the laboratory column. The boundary conditions for the computer model are described in Section 2.4.2.

2.4.2   Initial and Boundary Conditions

HYDRUS-1D simulations were completed with initial conditions corresponding to the laboratory soil column. For the draining event, the model was fully-saturated to represent the saturated laboratory soil column. The bottom boundary was specified as a variable pressure head representing the observed water table from the laboratory soil column. The top boundary condition was a constant flux with zero flux representing no addition of water since the laboratory soil column was covered on the top to shut off any evaporation and it was allowed to drain. This set-up was used to calibrate the HYDRUS

model against the observed soil moisture data. For the wetting events, the top boundary condition was specified to be *Atmospheric BC with Surface Layer*. A time series of applied wetting pulses was supplied as the top boundary condition, representing the volume of water added to the laboratory column.

2.4.3   Soil Hydraulic Parameters

The soil hydraulic parameters used to define the water retention curve were obtained by fitting the van Genutchen model to the observed soil moisture data and tensiometer data as described in Section 2.3.2. The values of these parameters are given in Table 2.3. In addition to the soil hydraulic properties defining the soil water retention curve, the saturated hydraulic conductivity (K_s) of the soil was specified to be equal to that of the laboratory soil column (0.172 cm/min, 2.5 m/day) as described in Section 2.3. This value was used to calibrate the HYDRUS-1D model to the observed soil column soil moisture. Later, the K_s was varied over an order of magnitude to simulate different soils along with a variation in the intensity of the applied pulse as the top boundary condition.

2.4.4   Calibration

The model was calibrated against the observed soil moisture data from the laboratory soil column. The modeled soil moisture for multiple depths from a draining event is shown against the observed soil moisture data from the laboratory soil column in Figure 2.12. The simulated soil moisture for 16 locations corresponding to the soil moisture sensor location in the laboratory column reasonably matched with the laboratory soil moisture data.
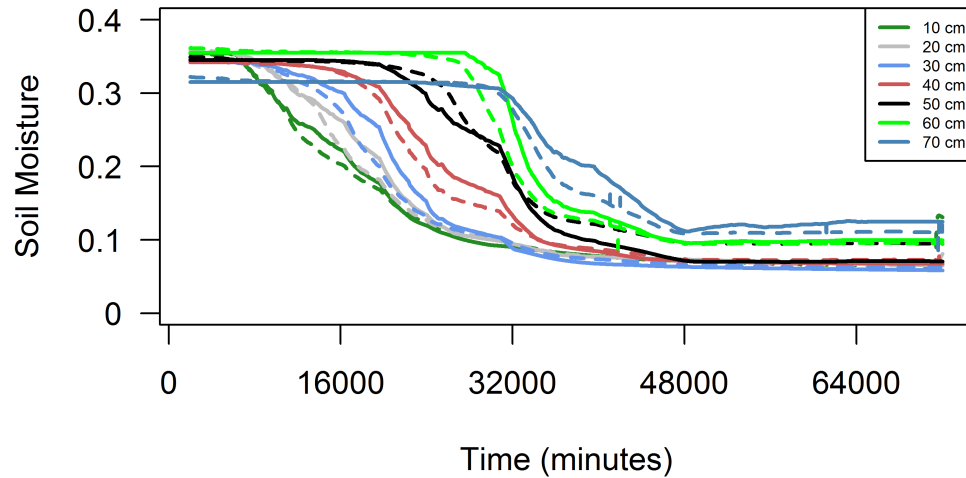
Figure 2.12: Model Calibration showing the modeled soil moisture (solid) against the observed soil moisture (dashed) from the laboratory soil column for draining event. Data from the top seven sensors is plotted against the modeled data.

2.4.5 Data for Model Development

After calibrating the model to the observed soil moisture data, the simulated soil column was extended in length by making if deeper from the original 160 cm to 1000 cm to allow simulations on a deeper (500 cm) depth to water table (DTWT) setting. This setup was used to generate data to develop the simplifying relationships described in Chapter 3. For multiple sets of applied rainfall volume, the soil hydraulic conductivity was varied over an order of magnitude higher and lower than the saturated hydraulic conductivity of the laboratory soil column described in Section 2.3. This is described in detail in Section 3.2.

2.5 Summary

This study used the field study site to get a preliminary analysis of the time scale of the wetting front propagation. Then, a laboratory soil column was designed to mimic the soil properties of the Myakka sand found in the field study site. The data from this laboratory soil column were used to calibrate a HYDRUS-1D computer model to run simulations with
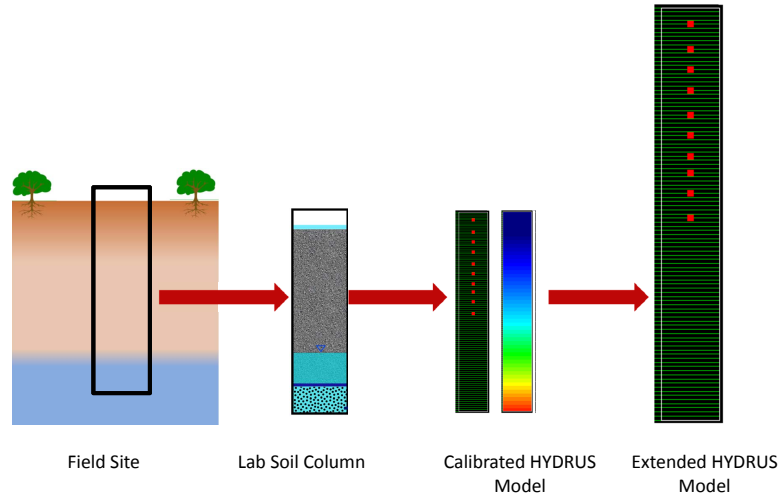
Figure 2.13: Schematic diagram showing the sources of Field, Laboratory and Numerical simulation data for this study. Table 2.5 lists the benefits and weaknesses of each data source

varying soil properties and rainfall intensities (top boundary condition) (Figure 2.13). The benefits and weaknesses of the three data sources (Field, Laboratory, Numerical simulations) are listed in Table 2.5. This table also lists the use and significance of each data source in this study.

Table 2.5: Benefits and weaknesses of the data sources used for developing recharge model. The specific use of each data source is also listed.

Source	Benefits	Weaknesses	Use in this study
Field Study	1. Natural undisturbed conditions 2. Multiple point scale observations along a transect 3. Includes root zone and heterogeneities	1. No control over the applied rainfall fluxes 2. No control over the ET processes 3. Rootwater uptake interferes with the study of time-scale of recharge	1. Preliminary analysis of time scale of wetting front propagation 2. Soil properties (Myakka sand) used to design laboratory soil column
Laboratory Soil Column	1. Controlled conditions 2. Easier installation of instrumentation (tensiometers, soil moisture, water table) 3. Soil properties similar to the field study area 4. No ET or rootwater uptake interference for studying wetting front propagation 5. Control over applied 'rainfall'	1. Difficult to change soil type/properties 2. Wetting/drying may take weeks to months 3. Maintenance and operation needs resources 4. Absence of ET or rootwater uptake 5. Limited maximum depth to water table	1. Study wetting front propagation for time scale of recharge 2. Soil moisture and tensiometer data used for calibration of HYDRUS-1D model 3. Soil properties (K_s, water retention curve) used to determine starting hydraulic properties for HYDRUS-1D simulations
Model Simulations	1. Easy to run rigorous simulations on different soil type/properties 2. Easy to vary applied 'rainfall' volume and intensities 3. Faster and easier than field data and laboratory data collection 4. Depth of the column can be varied easily to study deeper water table environments	1. Simplified representation of the natural conditions 2. Requires calibration or other source for defining van Genutchen parameters	1. Rigorous testing with different soil parameters and applied 'rainfall' volumes and intensities 2. Output data used to understand and generalize models for timing and quantity of recharge

Chapter 3 Model Development

Chapter 2 describes a preliminary analysis of time scale of recharge using the high resolution soil moisture data and water table data from the ECO area field study site. The laboratory soil column was constructed to represent the properties of Myakka soil found in the field study site. The high resolution soil moisture data from the laboratory soil column was used to calibrate the HYDRUS-1D model. This calibrated HYDRUS-1D model was modified by increasing its length to simulate water table conditions deeper than the laboratory soil column. This computer model was then used to run multiple simulations on an array of soil properties and a wide range of the intensity and volume of applied event (Table 3.1). The data from these simulations were used to develop two generalized models for normalized arrival time of the recharge and the amount of relative recharge. An overview of the data analysis methodology is represented by the flowchart in Figure 3.1.

3.1 Theoretical Background

Unsaturated flow in porus media can be described by Richards' equation (Equation 3.1), developed by extending Darcy's law by considering the unsaturated hydraulic conductivity (K) as a function of the *matric suction head* (ψ) or *soil moisture* (θ) [Richards, 1931]. Richards' Equation for one dimensional vertical flow (z coordinate direction) takes the form of Equation 3.2. This form is widely used to represent vertical unsaturated zone flow with gravity head and suction head.

$$\frac{\partial \theta}{\partial t} = \nabla . \left[K \left(\psi \right) \nabla \left(\psi - z \right) \right] \qquad (3.1)$$
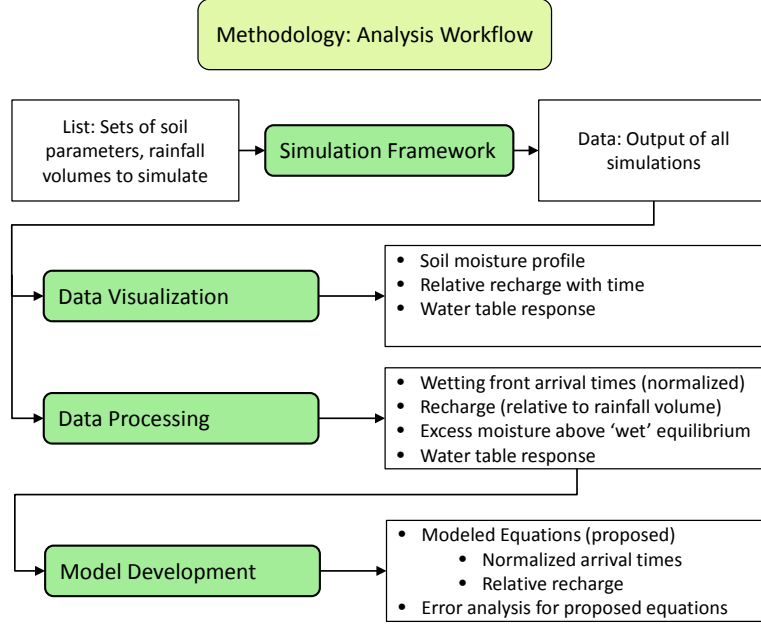
Figure 3.1: Flow chart of the methodology to develop the model. Framework used to visualize and process simulation data.

where ∇ is vector differential operator, ψ is the *matric suction head* (negative for unsaturated conditions due to capillary forces) and z is the *gravity head*.

$$\frac{\partial \theta}{\partial t} = \frac{\partial}{\partial z}\left[K(\theta)\left(\frac{\partial \psi}{\partial z} + 1\right)\right] \tag{3.2}$$

Flow of water in unsaturated soil involves important processes like plant root water uptake and groundwater recharge beyond the root zone. Unsaturated flow, as represented by the Richards' equation, is driven by complex relationships between soil moisture, the corresponding hydraulic conductivity, and matric suction. These relationships are nonlinear, expensive and difficult to estimate in laboratory or field conditions (discussed further in Section 3.1.1). Richards' equation does not have a closed-form analytical solution and is approximated using numerical methods by dividing the flow domain into discrete finite elements of finite difference grids. A computer model, HYDRUS-1D, developed by Šimůnek et al. [2005] solves Richards' equation in one dimension by numerical approximation using

26

finite element method to simulate the one-dimensional movement of water, heat, and solutes in unsaturated soil. HYDRUS-1D requires user defined relationships between soil moisture retention, conductivity and suction head. This computer model was used in this study to simulate unsaturated flow to study the timing and quantity of recharge.

3.1.1 Water Retention Curve

Richards' equation described in Section 3.1 requires functions relating soil moisture, hydraulic conductivity and matric suction. A curve relating the matric suction and the water content is called the Water Retention Curve (WRC) or Soil Moisture Characteristic Curve (SMCC). Several parametric equations exist to define water retention curves for soil. The parameters for such equations are empirical coefficients defining the shape of the curve for different soils. In this study, a function given by van Genuchten [1980] was used for the water retention curve (Equation 3.3). The pore-size distribution model proposed by Mualem [1976] was used for the unsaturated hydraulic conductivity function as given by Equation 3.4 [Šimůnek et al., 2005]. Used together, these relations are called the van Genutchen Mualem model (VGM) [Šimůnek et al., 2005]. The parameters like θ_r in the VGM model are not truly physical properties but rather variables for fitting observed retention curves. However, users frequently refer to the approximate analogy to physical soil state definitions (*e.g.* residual referred to as wilting point). Also, the van Genutchen Mualem model was found to be more reliable in the wet range than the dry range [Stephens and Rehfeldt, 1985; Ward et al., 1983].

$$\theta\left(\psi\right) = \theta_r + \frac{\theta_s - \theta_r}{\left[1 + \left(\alpha\left|\psi\right|\right)^n\right]^m} \qquad (3.3)$$

$$K\left(\psi\right) = K_s\Theta^l\left[1 - \left(1 - \Theta^{1/m}\right)^m\right]^2 \qquad (3.4)$$

where n is pore-size distribution index, $m = 1 - 1/n$, α is inverse of air-entry (bubbling) pressure head, the head at which suction begins to dominate, l is pore connectivity parameter (0.5, empirical estimation) and Θ is the *Effective Saturation* defined by Equation 3.5.

$$\Theta = \frac{\theta\left(\psi\right) - \theta_r}{\theta_s - \theta_r} \tag{3.5}$$

where θ_s is the saturated water content of the soil and θ_r is the residual water content.

3.1.2   Equilibrium Moisture Profile and Specific Yield

The specific yield has been defined differently but is generally considered to be the volume of water released from or held by the aquifer per unit change in water table depth [Freeze and Cherry, 1979; Todd, 1959]. In application of soil models, this definition assumed a constant value which has been found to be inaccurate in shallow water table conditions. Multiple studies have highlighted the variability is specific yield and have offered varying relationships to address this variability [Barlow et al., 2000; Jayatilaka and Gillham, 1996; Nachabe, 2002; Said et al., 2005; Shah and Ross, 2009]. A closed-form analytical expression for transient specific yield is available that related water table fluctuation to the amount of water released assuming equilibrium moisture content [Nachabe, 2002]. However, Shah and Ross [2009] showed through field and model simulations that it would actually vary considerably depending on the stress (ET, pumping, infiltration). Hence, assuming equilibrium moisture content in the shallow water table case is actually flawed.

The water content profile of a vertical soil column redistributes soil moisture after adding a volume of water on the top. The water content profile is said to reach *equilibrium* when the added volume redistributes and there are no net water fluxes in the soil column. At equilibrium, the moisture profile and the water table are stable. Any addition or removal

of water to this profile eventually results in redistribution of the soil moisture profile and the water table moves accordingly.

Field studies and HYDRUS-1D simulations have established that the equilibrium moisture content can vary between a *'dry' equilibrium* state and a *'wet' equilibrium* state (Figure 3.2) without a perceptible change in the water table elevation [Rahgozar, 2006; Shah and Ross, 2009]. When water is removed from the soil with moisture profile wetter than the 'dry' profile, the soil moisture redistributes to a stable 'dry' profile before a drop in the water table is observed. Similarly, when water is added to the soil with moisture profile drier than the 'wet' profile, it redistributes to a stable 'wet' profile before a rise in the water table is observed. The region between the 'dry' and 'wet' profile results in a variability in unsaturated zone storage. In this study, the model simulations started with a wetting pulse to create wet antecedent moisture conditions. This wetting pulse was then followed by seven different event pulses in different model runs. The intensities of these events (Event A through Event G) are given in Table 3.1.

The equilibrium water table corresponding to the applied volume can be calculated by solving the equation that equates the applied volume to the difference in the area under the curve for the water retention curves corresponding to the initial and the final water table configuration (Figure 3.3 and Equation 3.6).

$$Volume_{added} = \left[\int_0^{DTWT_2} VG_{WT2} - \int_0^{DTWT_1} VG_{WT1} \right] + \theta_s \left[WT_2 - WT_1 \right] \qquad (3.6)$$

where $Volume_{added}$ is the amount of water added to the soil column, VG_{WT1} and VG_{WT2} are the van Genutchen equations for the equilibrium profile corresponding to water tables WT1 and WT2, respectively.

Equation 3.6 can be solved by integrating the van Genutchen equation in the following manner:
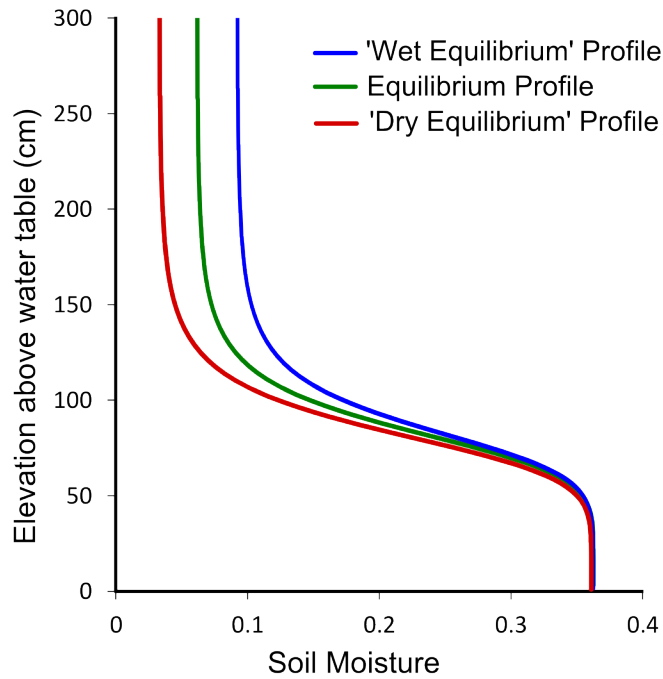
Figure 3.2: Conceptual representation of the *wet equilibrium* and *dry equilibrium* moisture content profiles. The region between the *wet* and *dry* equilibrium represent the variability in specific yield.
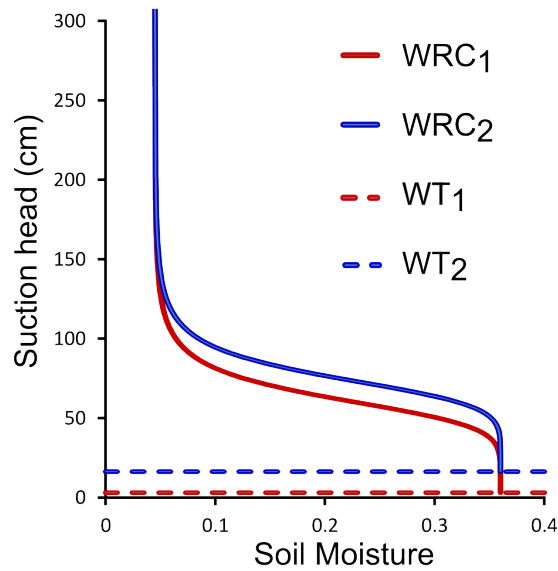
Figure 3.3: Calculation of the new water table elevation at equilibrium water retention. The shaded area corresponds to the volume of water added to the profile.

$$\int \theta(\psi)d\psi = d = \psi \left((\theta_s - \theta_r) \; _2F_1 \left(m, \frac{1}{n}; 1 + \frac{1}{n}; -(\alpha\psi)^n \right) + \theta_r \right) + constant$$

$$= \psi \left(\theta_r + (-\theta_r + \theta_s) \; _2F_1 \left(m, \frac{1}{n}; 1 + \frac{1}{n}; -(\alpha\psi)^n \right) \right)$$

$$= \psi\theta_r - \psi\theta_r \; _2F_1 \left(m, \frac{1}{n}; 1 + \frac{1}{n}; -(\alpha\psi)^n \right)$$

$$+ \psi\theta_s \; _2F_1 \left(m, \frac{1}{n}; 1 + \frac{1}{n}; -(\alpha\psi)^n \right)$$

(3.7)

where $_2F_1$ is Gauss' Hypergeometric function.

The script (coded in Python language) to solve this equation has been provided in Appendix C. This solution can be used to find the equilibrium water table configuration for a known volume of water added to the soil column. Hence, the water table fluctuation can be used to quantify recharge as a fraction of total applied pulse, indicating the extent of relative recharge to the water table.

3.1.3   Effective Pulse Volume: P_{vol}

As described in the Section 3.1.2, a 'wet' equilibrium moisture profile is required for recharge to take place following a rainfall event. A part of the actual applied pulse volume ($P_{applied}$) is required to move the initial moisture profile to a wet equilibrium state. The effective pulse volume (P_{vol}) can be defined as the amount of pulse volume that is responsible for groundwater recharge after satisfying the unsaturated zone storage difference between the 'wet' and *antecedent soil moisture profile* (Equation 3.8). This definition of P_{vol} is used later to calculate θ' for developing the proposed models in Section 3.3.1.

$$P_{vol} = P_{applied} - \int_{z=0}^{z=d} (\theta_w - \theta_i) \, dz$$

(3.8)

where d is the depth at which the recharge is calculated, θ_w is the 'wet' equilibrium moisture profile and θ_i is the initial or antecedent moisture profile.

3.1.4 Relative Recharge: R'

Groundwater recharge is quantified as the amount of water that reaches the water table after a pulse of rainfall volume is applied to top of the soil column. However, this is overly simplistic as the unsaturated flow actually only has to reach to the top of the capillary zone to cause the water table to rise [Said et al., 2005]. In sandy soils, such as those used in the laboratory soil columns, the capillary zone is approximately 1 m above the water table [Shah and Ross, 2009; Trout and Ross, 2006]. In this study, recharge (R) was normalized by the applied pulse volume (P_{vol}) and it was termed *Relative Recharge* (Equation 3.9). Relative recharge at a given depth can be defined as the volume of applied pulse that has recharged beyond that depth divided by the total volume of the applied pulse. The value of relative recharge (R') at a given depth (d) varies from 0 to 1. Relative recharge at a depth is 0 when the entire pulse volume is above that depth and the wetting front has not yet reached that depth. Relative recharge at a depth is 1 when all of the applied pulse volume makes it past that depth. This definition is used to develop the model for the predicting recharge given in Section 3.3.2.

$$R'_d = \frac{P_{vol} - \int_0^d \left(\theta_{pulse} - \theta_{eqbm} \right) dz}{P_{vol}} \tag{3.9}$$

where R'_d is the relative recharge at depth d, P_{vol} is the volume of the applied pulse, θ_{pulse} and θ_{eqbm} are the soil moisture profiles for the applied pulse and equilibrium, respectively.

3.2 HYDRUS Simulations

Model simulations were carried out over a wide range of soil properties and applied rainfall intensities using the HYDRUS-1D setup described in Section 2.4. For each model simulation case corresponding to a given set of soil properties, 8 model simulations were carried out by varying the intensity of the applied pulse. For each of these 8 model

Table 3.1: Applied rainfall intensities for events A through G and Ks multiplier for model simulation. Event 0 represents base simulation with a draining profile in the absence of an applied event.

Simulation Set	1	2	3	4	5	6	7	8	9	10	11
Ks multiplier[1]	0.12	0.2	0.3	0.4	0.5	0.7	1	1.5	2	5	10
Event 0[2]	0	0	0	0	0	0	0	0	0	0	0
Event A	1.2	1.0	1.7	1.7	1.3	1.4	2.6	3.9	2.1	1.3	1.0
Event B	2.4	2.1	2.4	2.1	2.6	2.2	5.2	7.7	4.1	2.6	2.1
Event C	3.6	4.1	3.4	2.9	3.9	3.6	7.7	11.6	6.2	5.2	5.2
Event D	6.0	6.2	6.7	4.1	5.2	5.1	10.3	15.5	10.3	7.7	10.3
Event E	8.4	10.3	10.1	8.3	6.5	7.2	12.9	19.4	14.4	10.3	15.5
Event F	12.0	14.4	16.8	12.4	7.7	14.4	15.5	23.2	16.5	15.5	20.6
Event G	18.0	20.6	23.6	20.6	10.3	21.7	20.6	31.0	20.6	25.8	25.8

[1] This factor was multiplied with Ks of soil column to get Ks for this simulation
[2] Events intensities in cm/hr

simulations in each simulation case, an initial wetting pulse with an intensity of 5.2 cm/hr was applied to simulate initial conditions of a 'wet' equilibrium described in Section 3.1. The second pulse was applied after 62 days of the first wetting pulse. The saturated hydraulic conductivity for each simulation case was determined by multiplying a factor with the saturated hydraulic conductivity of the laboratory soil column. For each simulation case, these factor multipliers are listed in Table 3.1 along with a set of 7 rainfall events with varying intensities (Event A through Event G). Event 0 represents the base simulation in which no second pulse was applied after the first wetting pulse. This base run was used to determine the change in soil moisture because of second pulse from the remaining 7 events (Event A through Event G). Hence, the difference between the simulation soil moisture from Even 0 (base event) and events A through G can be used to determine the effect of the corresponding events (Event A through Event G). The program to extract and analyze soil moisture and water table data from the model simulations is provided in Appendix D.

3.3   Development of Models

The data generated for a variety of rainfall intensities and K_s values from Section 3.2 were used to develop the simple models proposed in Sections 3.3.1 and 3.3.2. For each simulation set corresponding to a K_s value, a total of 8 HYDRUS simulations were done. Out of these 8 simulations, Event 0, was the the base simulation where a wetting pulse of 5.2 cm was applied over an hour at the start of the simulation and the model was allowed to run for 100 days. For the other 7 simulations, Event A through Event G (Table 3.1), the wetting pulse was applied as in Event 0 at the start of the simulation followed by another pulse at day 60. This was repeated for all K_s values for three different water retention curves. The output files from all the simulations were analyzed by the program listed in Appendix D to extract and analyze soil moisture and water table data. The soil moisture profile of the base event (Event 0) was subtracted from the soil moisture profile of each of event A through G to determine the excess soil moisture (θ') due to the second pulse (A through G). This excess soil moisture was used to calculate the time of arrival of wetting front at different depths as described in Section 3.3.1.

3.3.1   Model t_a: Wetting Front Arrival Time

For a given depth, the excess soil moisture of more than 1 percent was considered to be an indicator of the arrival of wetting front at that location. Soil moisture profiles corresponding to the wetting front arrival at 0.5 m intervals is shown in Figure 3.4 (a). For each of the 7 events (A through G), wetting front arrival time (t_a) was calculated using this approach for 10 cm depth intervals ranging from 10 cm to 400 cm below the top surface as shown in Figure 3.4 (b). It indicates that the arrival time is a function of the depth and the applied pulse volume.

However, to make the arrival time independent of the rainfall intensities (or pulse volume) the arrival time at a certain depth (d) was converted to a non-dimensional time
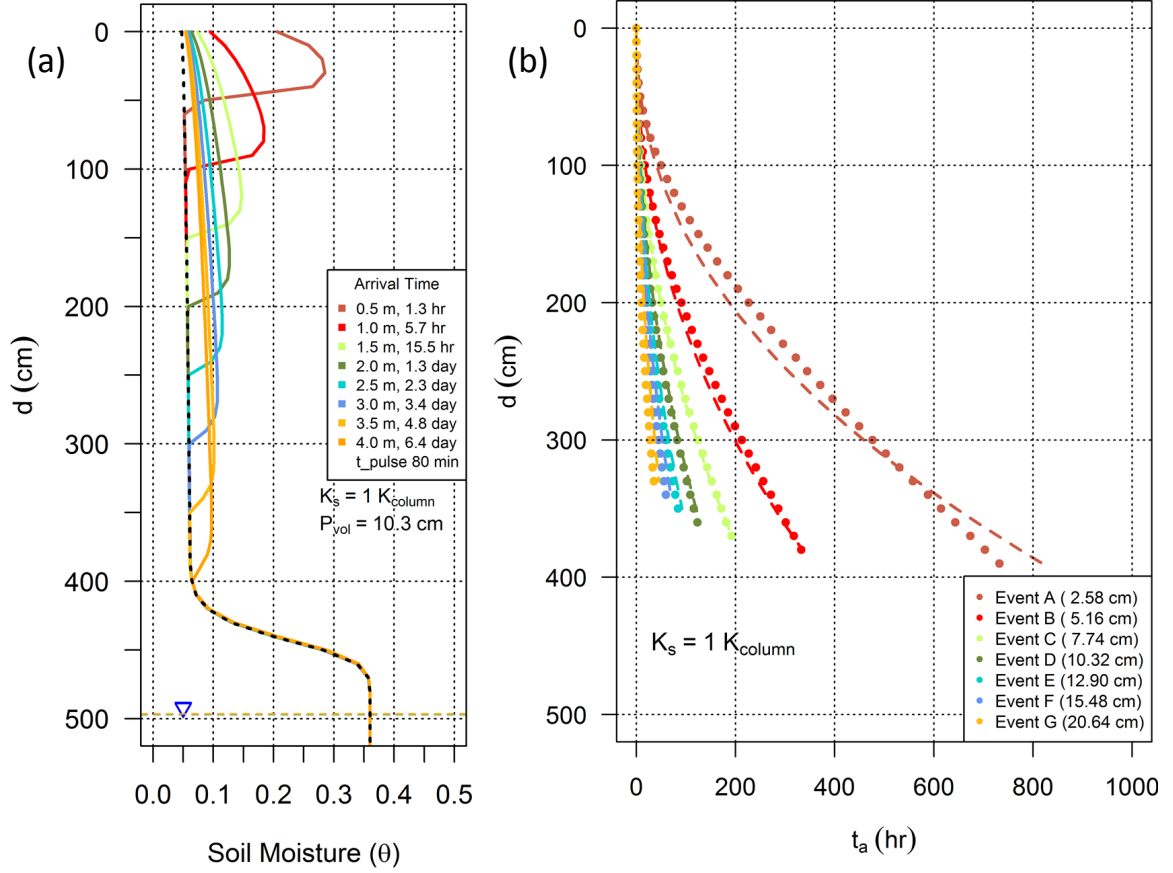
Figure 3.4: Soil moisture profile showing wetting front propagation through HYDRUS simulation of the soil column. (a) Wetting front arrival at 0.5 m intervals is shown (time of arrival, t_a is shown in legends). (b) Time of arrival, t_a for all events for simulation set 7 (Table 3.1).

(t_n) by dividing it by the corresponding depth (d) and again dividing it by the saturated hydraulic conductivity (K_s) as described by Equation 3.10.

$$t_n = \frac{t_a}{d/K_S} \tag{3.10}$$

The velocity at which the wetting front moves was found to be a function of the excess moisture content above the wet equilibrium water retention curve. As seen in Figure 3.5, the shape of the wetting front can be assumed to be approximately rectangular with dimensions of $\theta' \times depth$, integrated equal to the applied pulse volume (P_{vol}). Hence, the
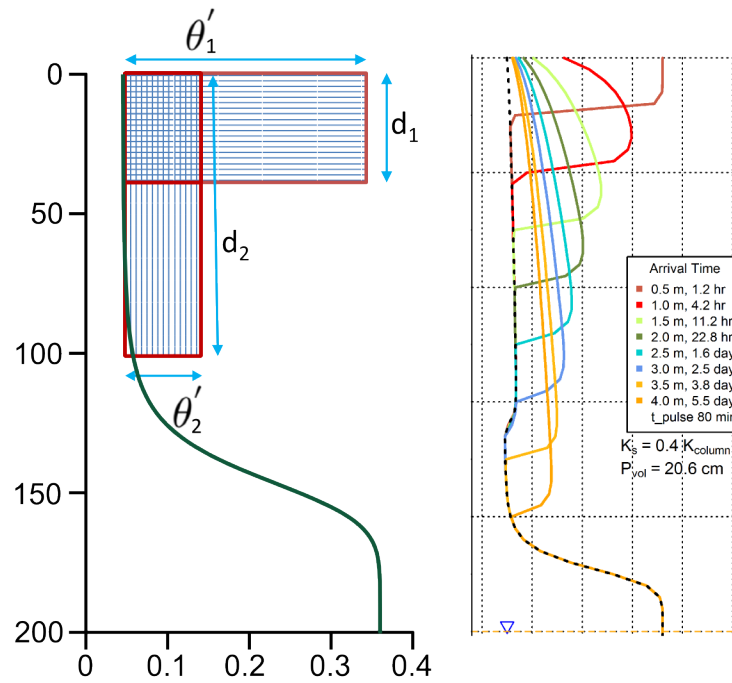
Figure 3.5: Assumption of rectangular and uniform wetting front (left) to calculate θ' at a given depth (d). HYDRUS-1D simulated moisture profile shows an approximately uniform rectangular wetting profile (right)

excess moisture content (θ') was determined by dividing the pulse volume (P_{vol}) by the depth (d) at which the arrival time is being calculated (Defined in Equation 3.12).

The non-dimensional time (t_n) becomes independent of the event intensity for a given simulation when plotted against the excess moisture content above the equilibrium (θ'), as shown in Figure 3.6 through Figure 3.16. A curve of the form given in Equation 3.13 can be fitted for a given simulation case with multiple events of varying intensity.

$$P_{vol} = \theta'_1.d_1 = \theta'_2.d_2 = \theta'.d \tag{3.11}$$

where θ'_1 and θ'_2 are the soil moisture contents corresponding to depths d_1 and d_2, respectively, as shown in Figure 3.5.

$$\theta' = \frac{P_{vol}}{d} \tag{3.12}$$

$$t_n = c_1 \, \theta'^{-\lambda} \tag{3.13}$$

The values of the fitted coefficients varied from 0.04 to 0.07 for various simulation sets corresponding to different pulse intensities given in Table 3.1. To simplify the equation, the coefficient was fixed at 0.05 and the equation was fitted to the data to estimate λ by minimizing the root mean square errors for predicting the non-dimensional time of arrival. This reduced Equation 3.13 to Equation 3.14.

$$t_n = 0.05 \, \theta'^{-\lambda} \tag{3.14}$$

The λ variable was found to be independent of the pulse intensities but dependent on the saturated hydraulic conductivity of the soil for the given simulation case. The value of λ was found to be related to the saturated hydraulic conductivity by another power law given by Equation 3.15.
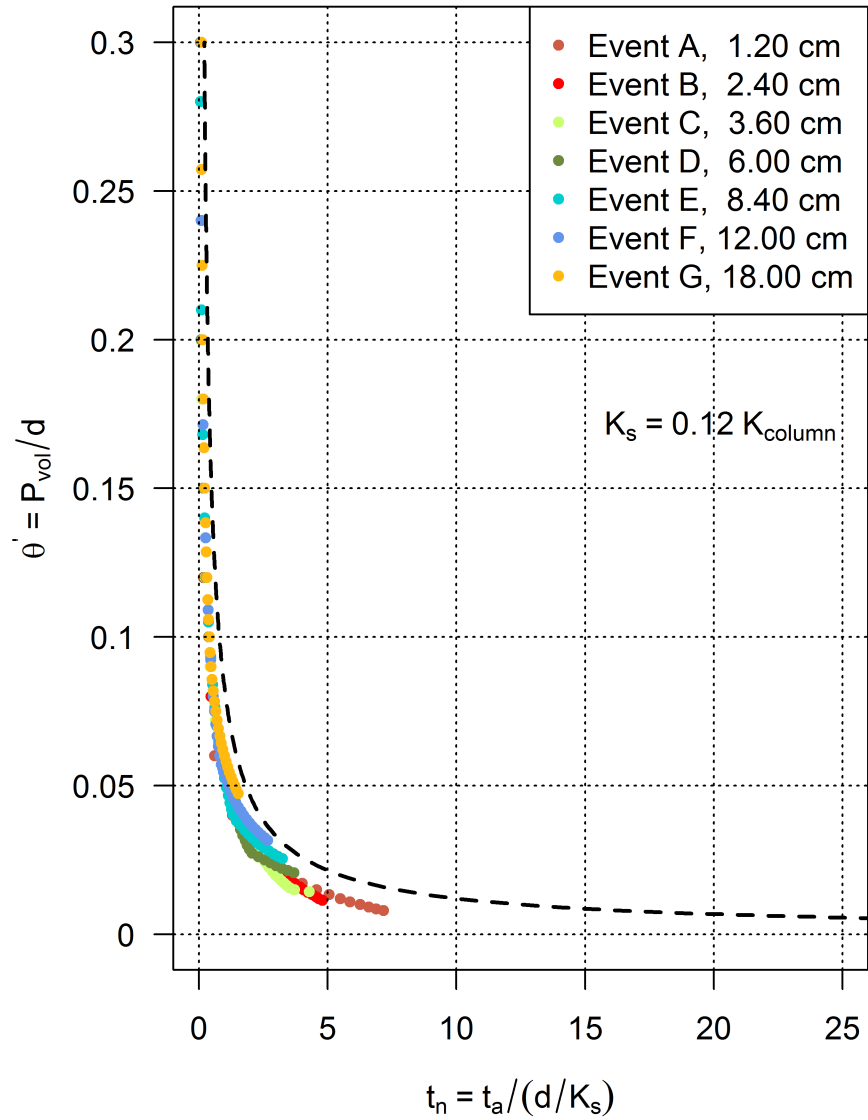
Figure 3.6: Normalized wetting front arrival time (t_n) for simulation set 1 (Table 3.1). Dashed line shows the model (Equation 3.13) fitted for all 7 events with $K_s = 0.12\ K_{column}$.
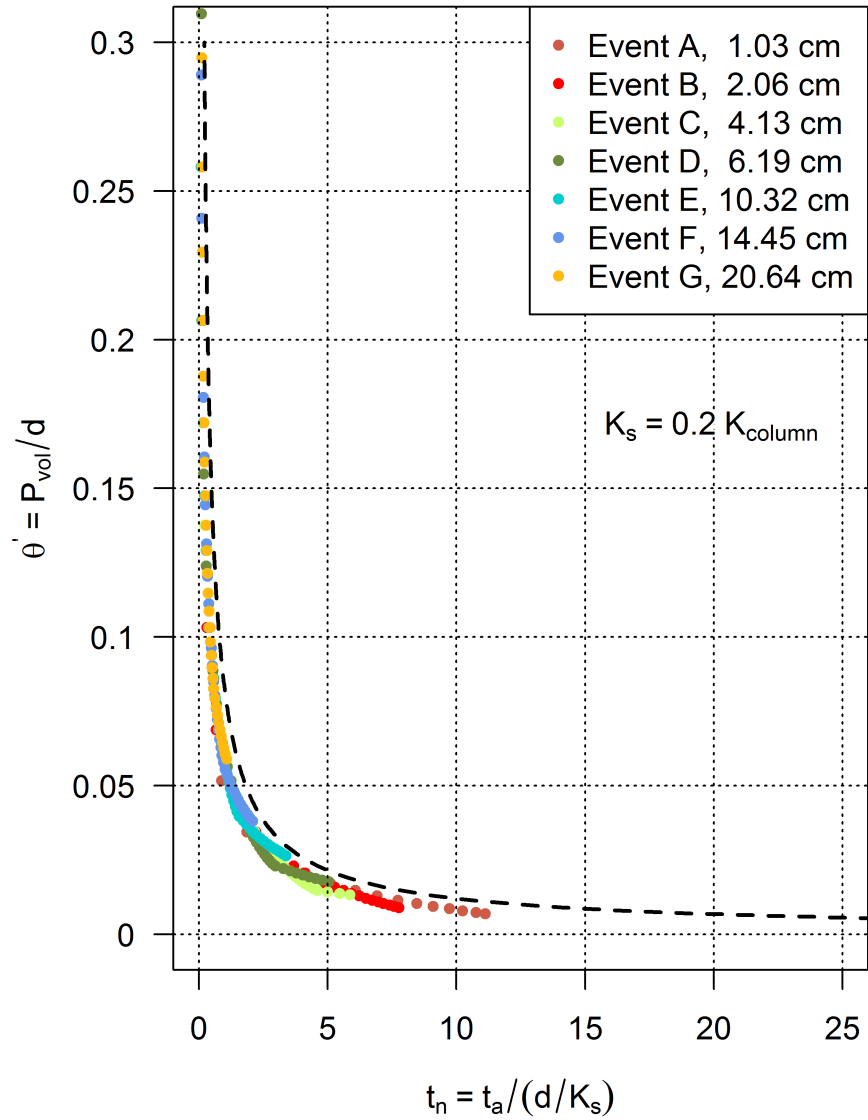
Figure 3.7: Normalized wetting front arrival time (t_n) for simulation set 2 (Table 3.1). Dashed line shows the model (Equation 3.13) fitted for all 7 events with $K_s = 0.2\ K_{column}$.
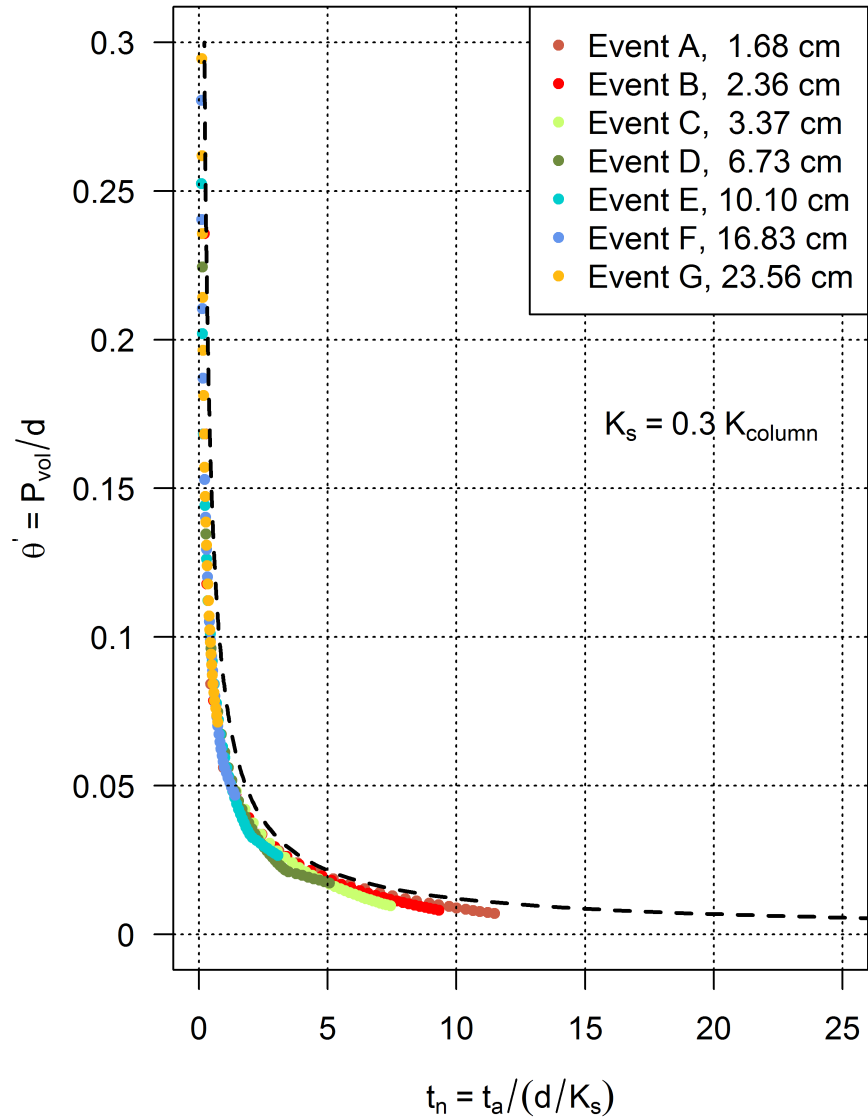
Figure 3.8: Normalized wetting front arrival time (t_n) for simulation set 3 (Table 3.1). Dashed line shows the model (Equation 3.13) fitted for all 7 events with $K_s = 0.3\ K_{column}$.
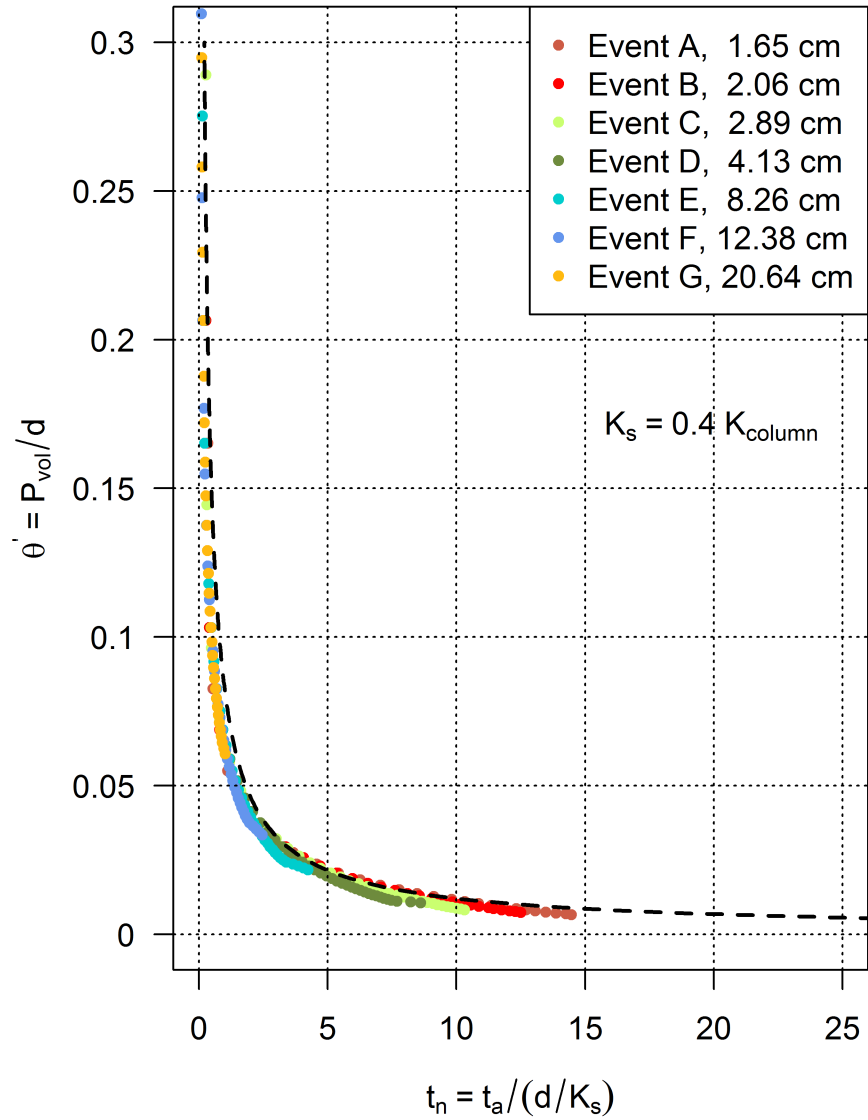
Figure 3.9: Normalized wetting front arrival time (t_n) for simulation set 4 (Table 3.1). Dashed line shows the model (Equation 3.13) fitted for all 7 events with $K_s = 0.4\ K_{column}$.
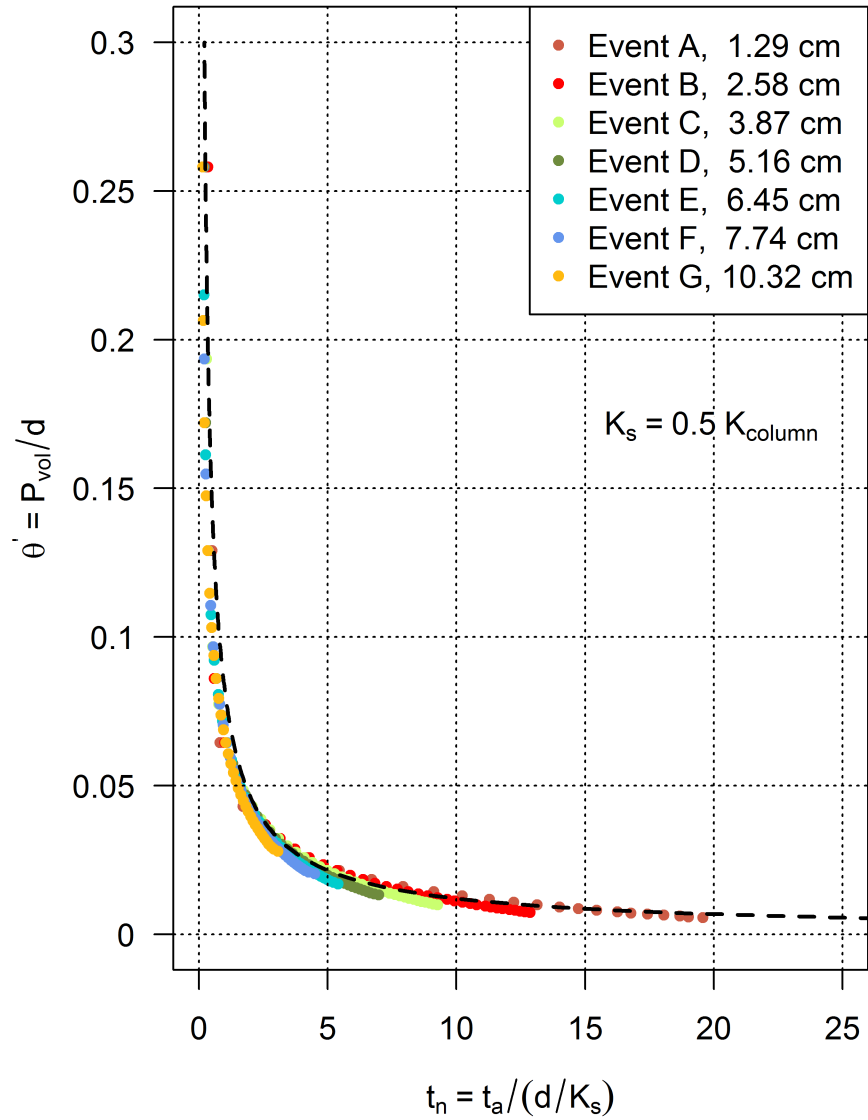
Figure 3.10: Normalized wetting front arrival time (t_n) for simulation set 5 (Table 3.1). Dashed line shows the model (Equation 3.13) fitted for all 7 events with $K_s = 0.5\ K_{column}$.
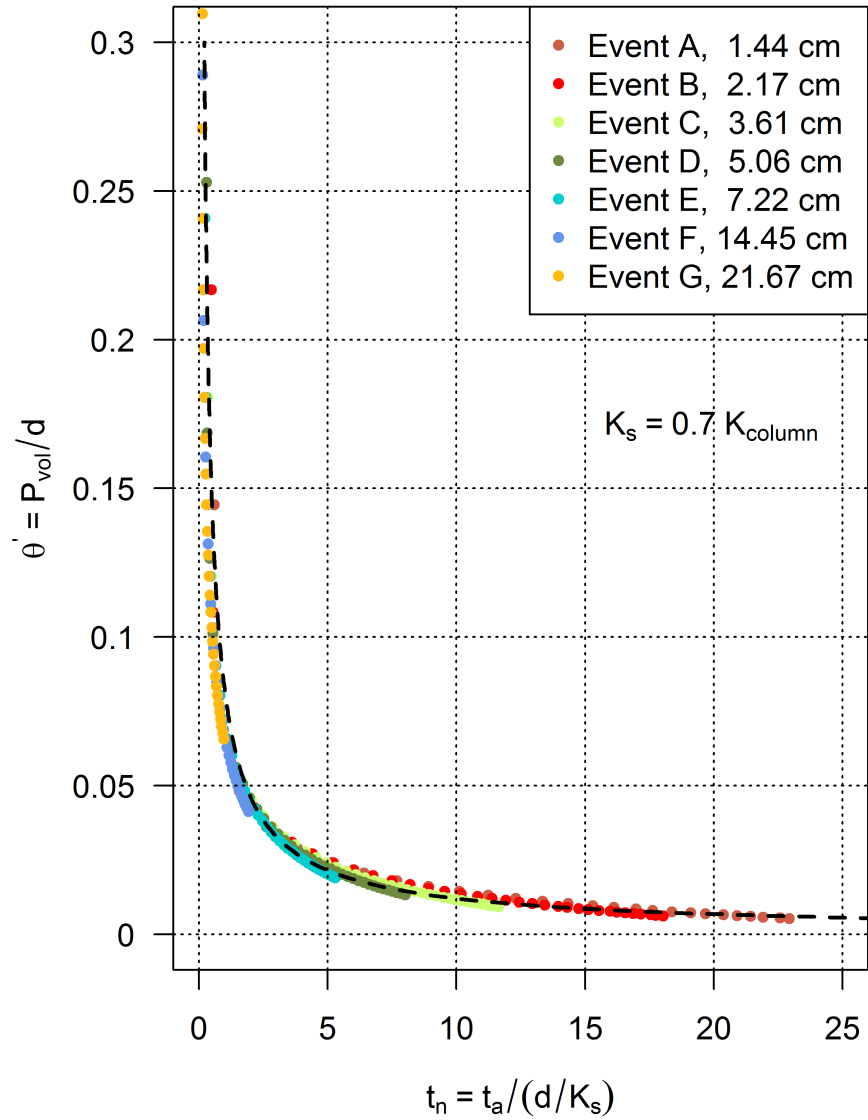
Figure 3.11: Normalized wetting front arrival time (t_n) for simulation set 6 (Table 3.1). Dashed line shows the model (Equation 3.13) fitted for all 7 events with $K_s = 0.7\ K_{column}$.
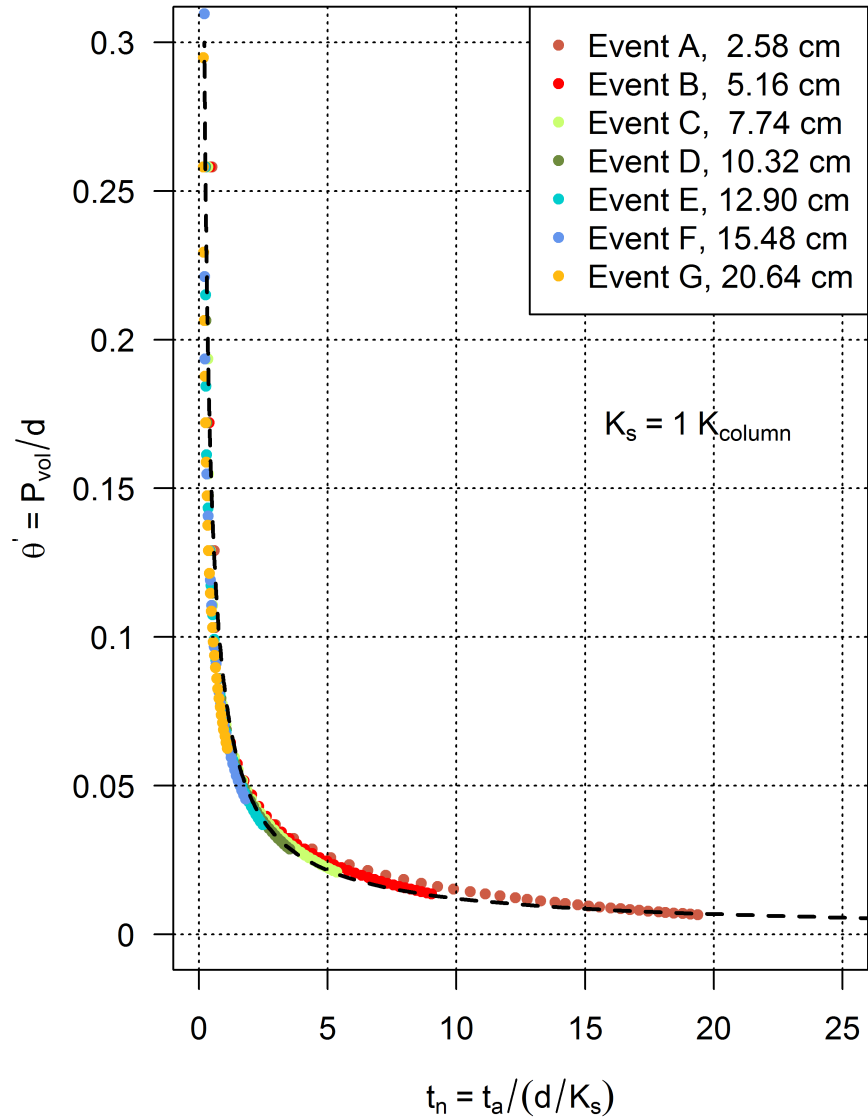
Figure 3.12: Normalized wetting front arrival time (t_n) for simulation set 7 (Table 3.1). Dashed line shows the model (Equation 3.13) fitted for all 7 events with $K_s = 1\ K_{column}$.
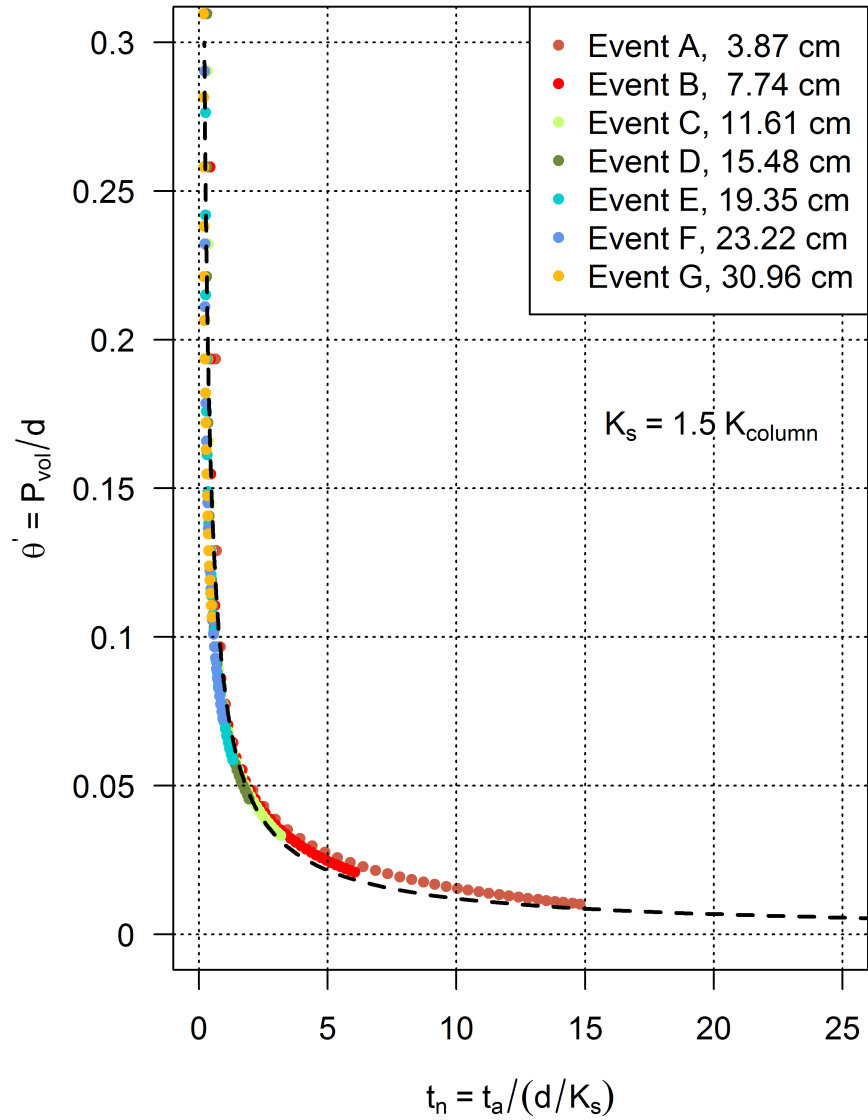
Figure 3.13: Normalized wetting front arrival time (t_n) for simulation set 8 (Table 3.1). Dashed line shows the model (Equation 3.13) fitted for all 7 events with $K_s = 1.5\ K_{column}$.
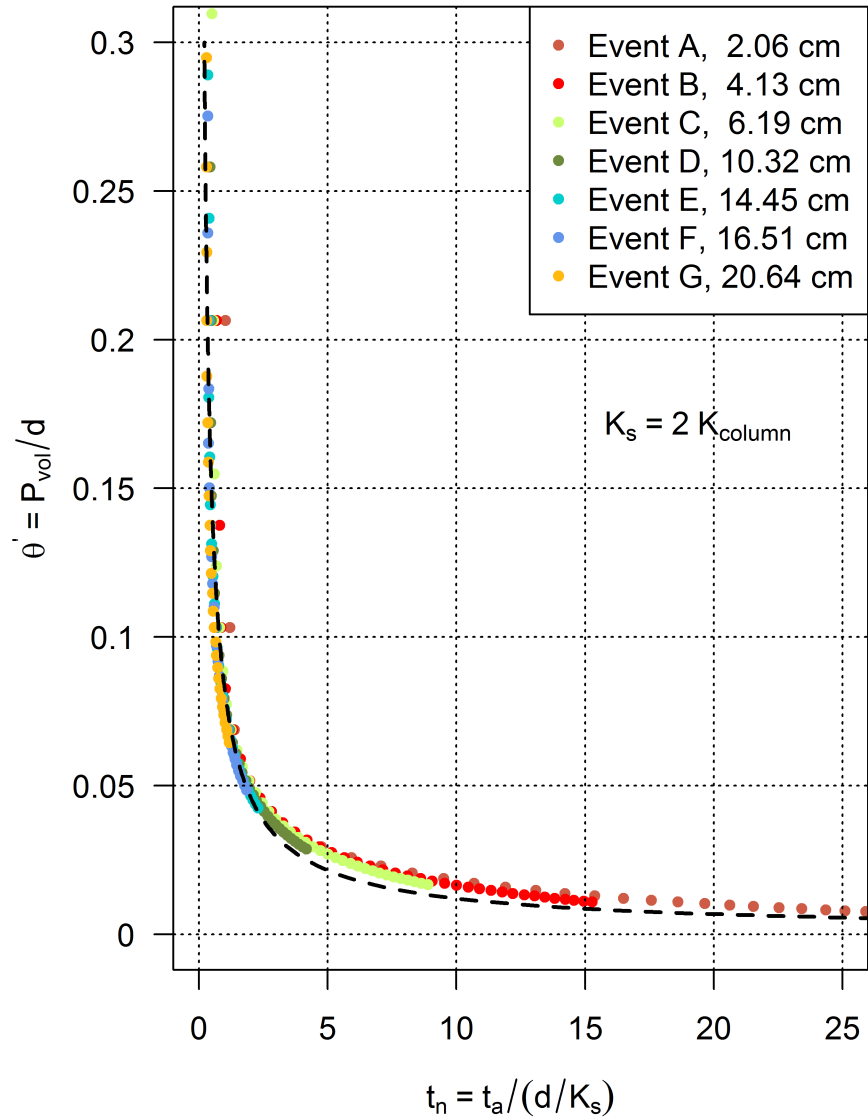
Figure 3.14: Normalized wetting front arrival time (t_n) for simulation set 9 (Table 3.1). Dashed line shows the model (Equation 3.13) fitted for all 7 events with $K_s = 2\ K_{column}$.
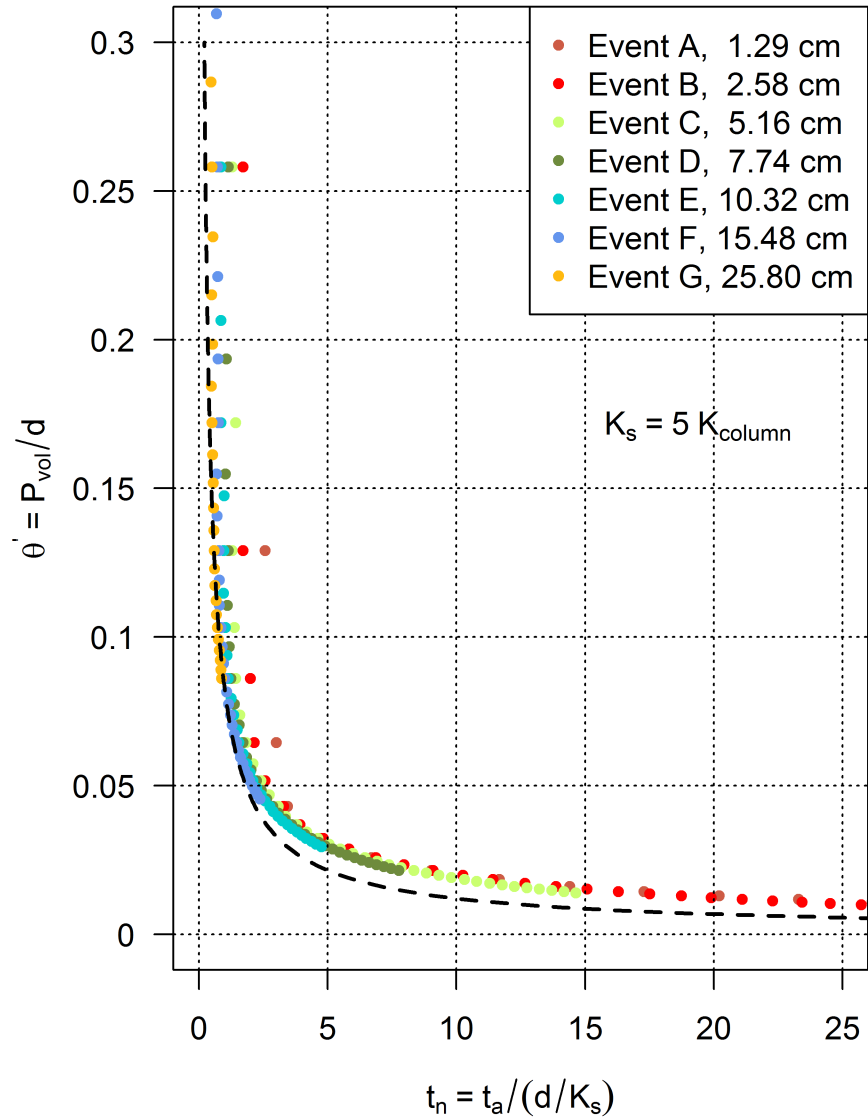
Figure 3.15: Normalized wetting front arrival time (t_n) for simulation set 10 (Table 3.1). Dashed line shows the model (Equation 3.13) fitted for all 7 events with $K_s = 5 \, K_{column}$.
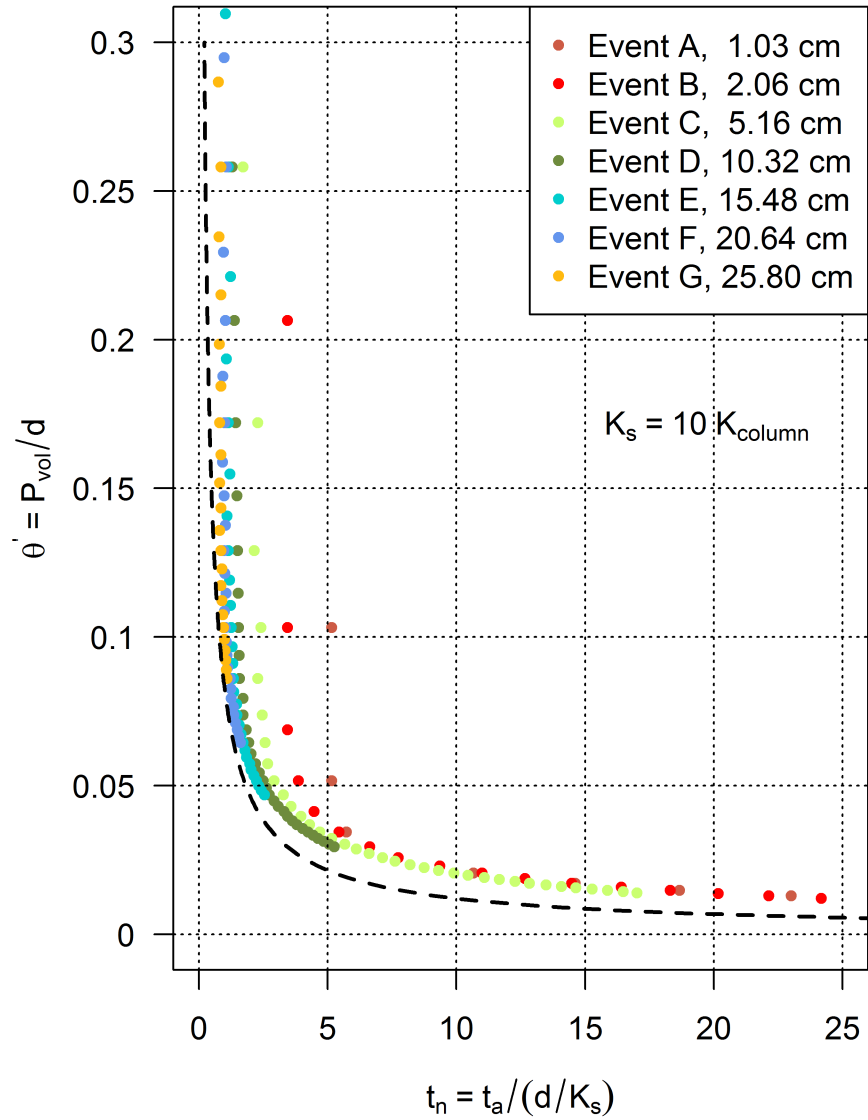
Figure 3.16: Normalized wetting front arrival time (t_n) for simulation set 11 (Table 3.1). Dashed line shows the model (Equation 3.13) fitted for all 7 events with $K_s = 10\ K_{column}$.
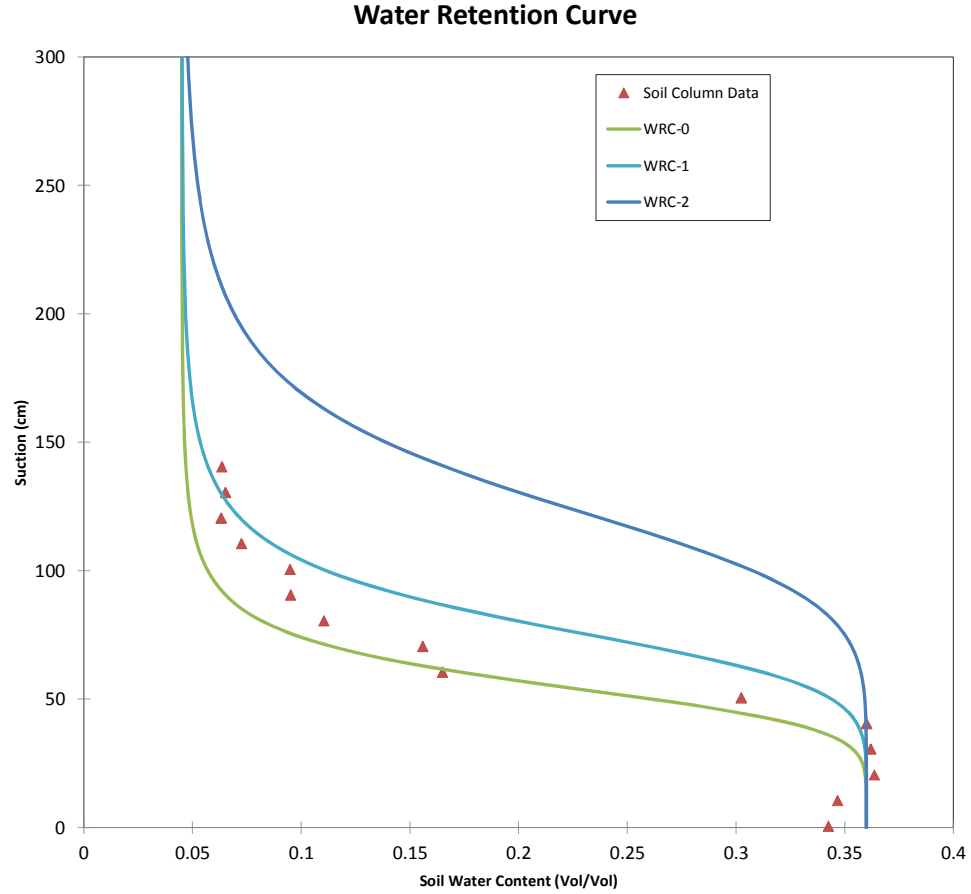
Figure 3.17: Range of water retention curves used for simulations. Tensiometer data from the laboratory soil column are also shown.

$$\lambda = c_2 \ K_s^{-0.06} \tag{3.15}$$

where the coefficient c_2 was found to be different for each water retention curve, defined by varying the van Genutchen parameter $alpha$ (α). The values of the coefficient c_2 are given in Table 3.2 for the WRCs used in this study to develop the models.

$$t_a = t_n \frac{d}{Ks} \tag{3.16}$$

Table 3.2: Coefficients for Equation 3.15 to calculate λ corresponding to the water retention curves (WRC) used in this study. The water retention curves used for simulations are shown in Figure 3.17

WRC used[1]	$alpha^2$	Coefficient c_2
WRC 0	0.018	1.334
WRC 1	0.013	1.331
WRC 2	0.008	1.28

[1] Water Retention Curve for simulation cases in table 3.1
[2] Van Genutchen Parameter

The time of arrival can be calculated from the predicted t_n using Equation 3.16. A discussion on the error in t_a predictions is provided in Chapter 4. The time scale of recharge for typical Myakka soils represented in this study can be estimated by using the model proposed in this section. The steps to estimate the time of arrival of the wetting front using the model discussed in this chapter are described in the Chapter 4.

3.3.2 Model R': Progression of Recharge

Time scale of recharge was calculated by the model proposed in Section 3.3.1. The quantity of recharge was calculated using the soil moisture and water table fluctuation data from the simulations described in Section 3.2. For a given depth (d), recharge was normalized to the total volume of the applied pulse as per Equation 3.17 and it was called relative recharge (R'_d) as defined in Section 3.1.4. Relative recharge at a given depth can be defined as the volume of applied pulse that has recharged beyond that depth divided by the total volume of the applied pulse. The value of relative recharge (R') at a given depth (d) varies from 0 to 1. Relative recharge at a depth is 0 when the entire pulse volume is above that depth and the wetting front has not yet reached that depth. Relative recharge equal to 1 occurs when all of the applied pulse volume makes it past that depth.

$$R'_d = \frac{P_{vol} - \int_0^d \left(\theta_{pulse} - \theta_{eqbm} \right) dz}{P_{vol}} \qquad (3.17)$$

50
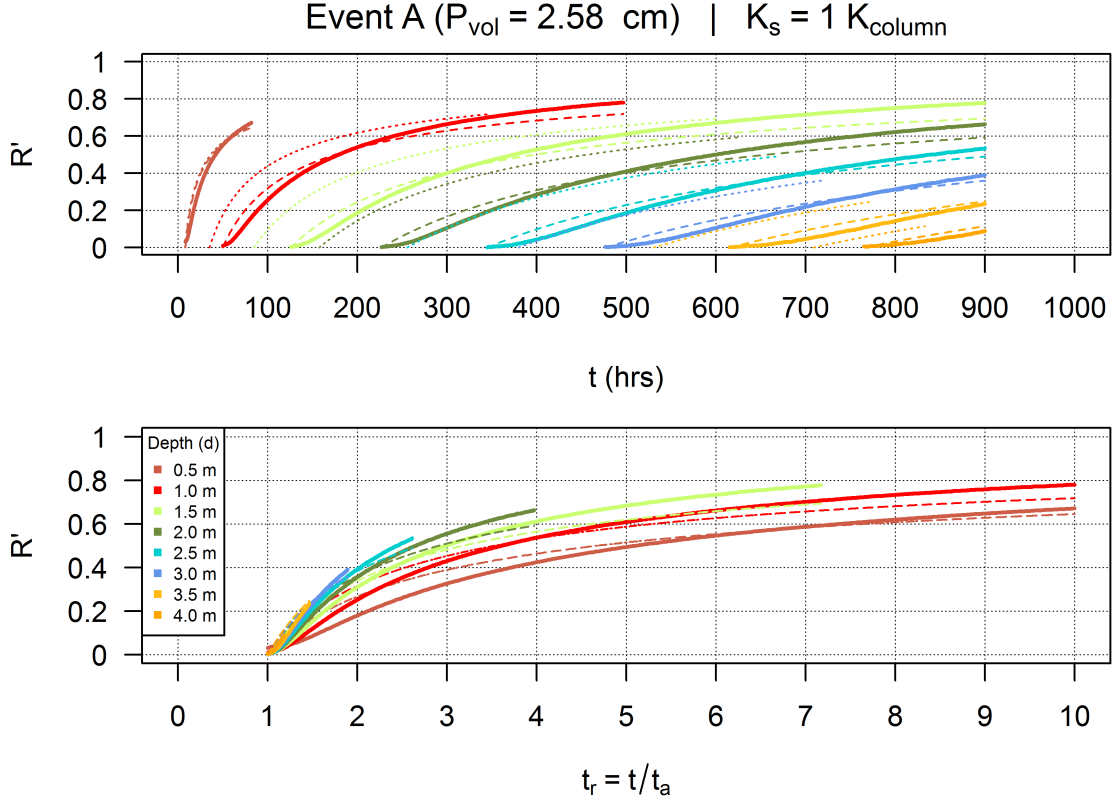
Figure 3.18: Model estimated relative recharge (R') at different depths for Event A from simulation set 7. (R') is plotted against time, t (top) and relative time, t_r (bottom). $K_s = 1 \ K_{column}$ as listed in Table 3.1.

where R'_d is the relative recharge at depth d, P_{vol} is the volume of the applied pulse, θ_{pulse} and θ_{eqbm} are the soil moisture profiles for the applied pulse and equilibrium, respectively.

For plotting relative recharge at given depth, relative time (t_r) was calculated by dividing model time (t) by the time of arrival (t_a) of the wetting front at that depth as given in Equation 3.18. The value of relative time is 1 for a given depth at the time when the wetting front just arrives at that depth (t_a, arrival time) and when the relative recharge just begins to become non-zero. This allowed for fitting a single model since the relative recharge is 0 for all depths when the relative time is 1 as shown in Figures 3.18 through 3.23.

51
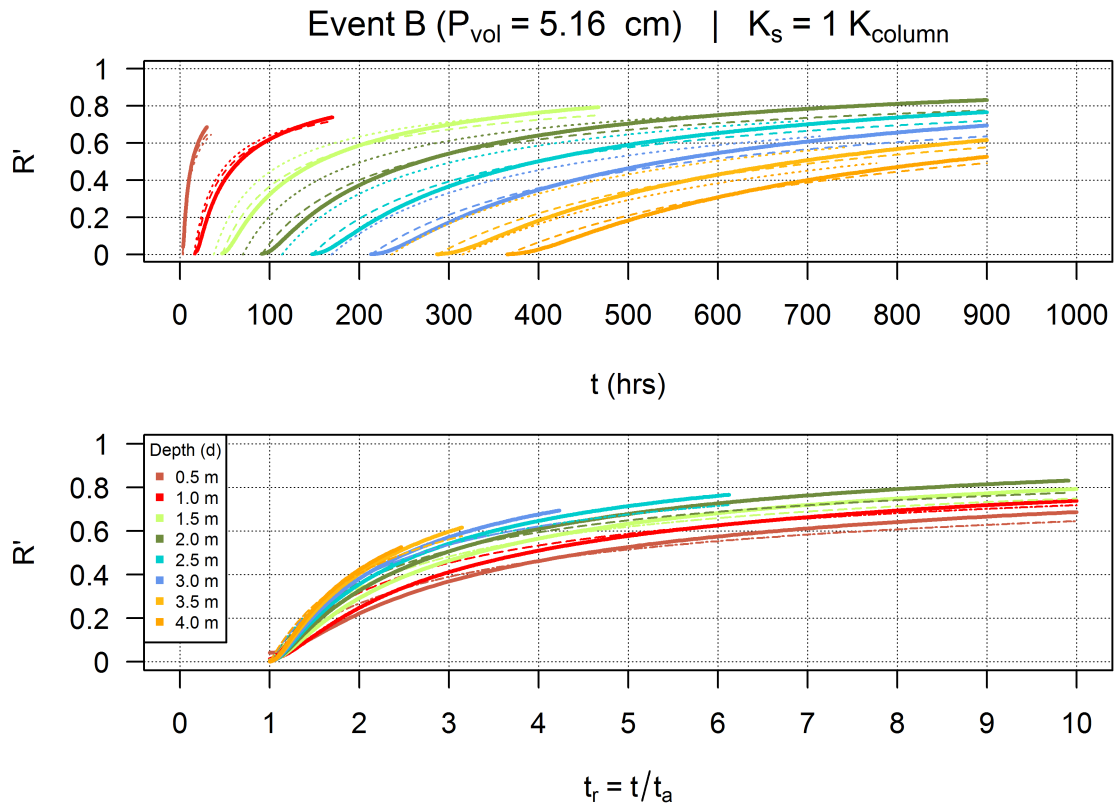
Figure 3.19: Model estimated relative recharge (R') at different depths for Event B from simulation set 7. (R') is plotted against time, t (top) and relative time, t_r (bottom). $K_s = 1 \ K_{column}$ as listed in Table 3.1.
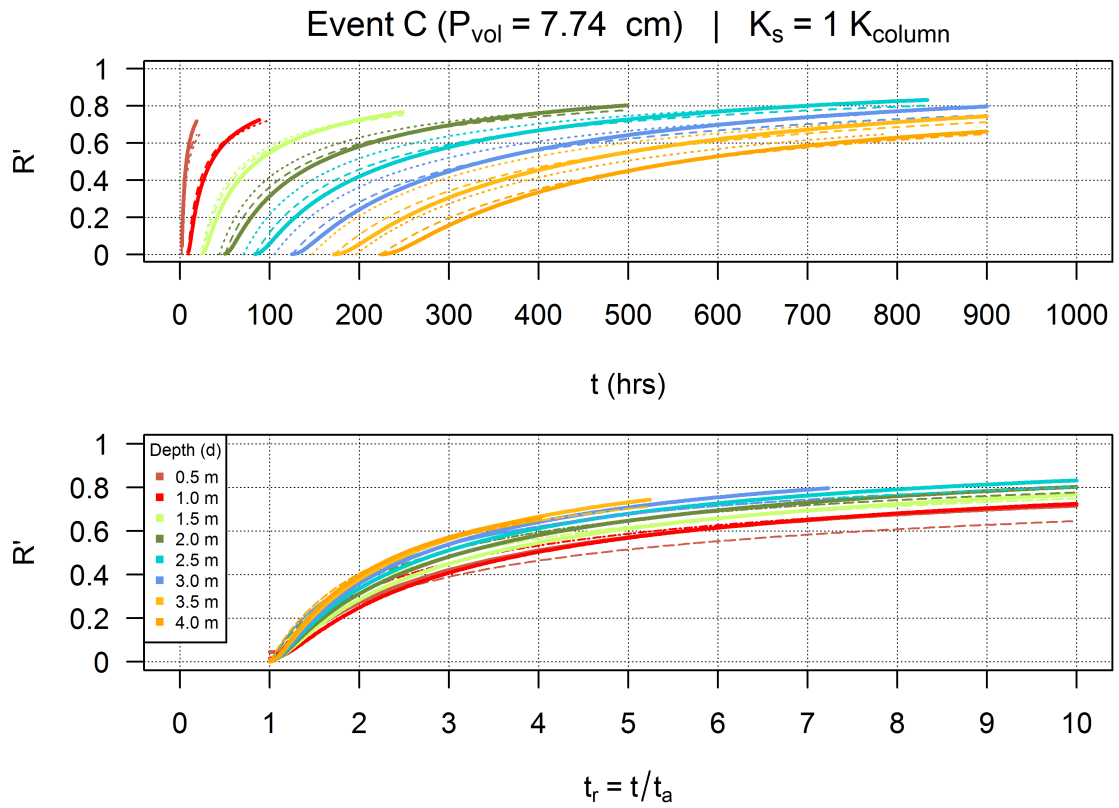
Figure 3.20: Model estimated relative recharge (R') at different depths for Event C from simulation set 7. (R') is plotted against time, t (top) and relative time, t_r (bottom). $K_s = 1\ K_{column}$ as listed in Table 3.1.
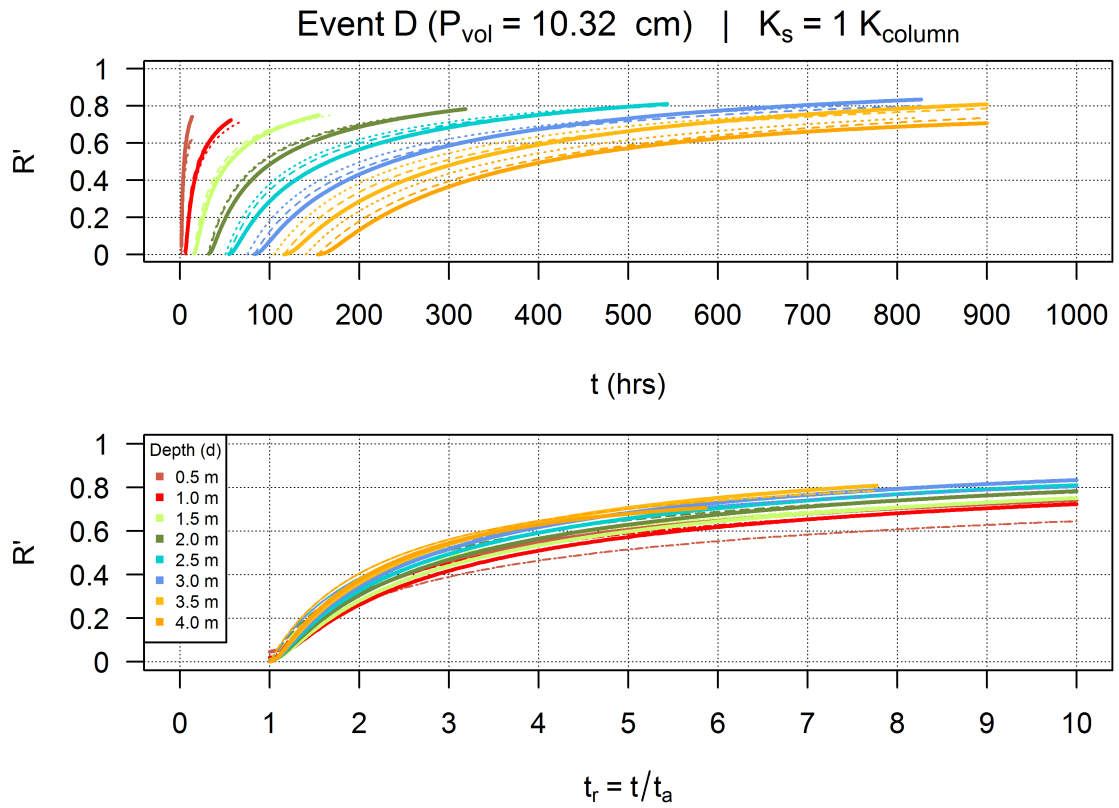
Figure 3.21: Model estimated relative recharge (R') at different depths for Event D from simulation set 7. (R') is plotted against time, t (top) and relative time, t_r (bottom). $K_s = 1\ K_{column}$ as listed in Table 3.1.
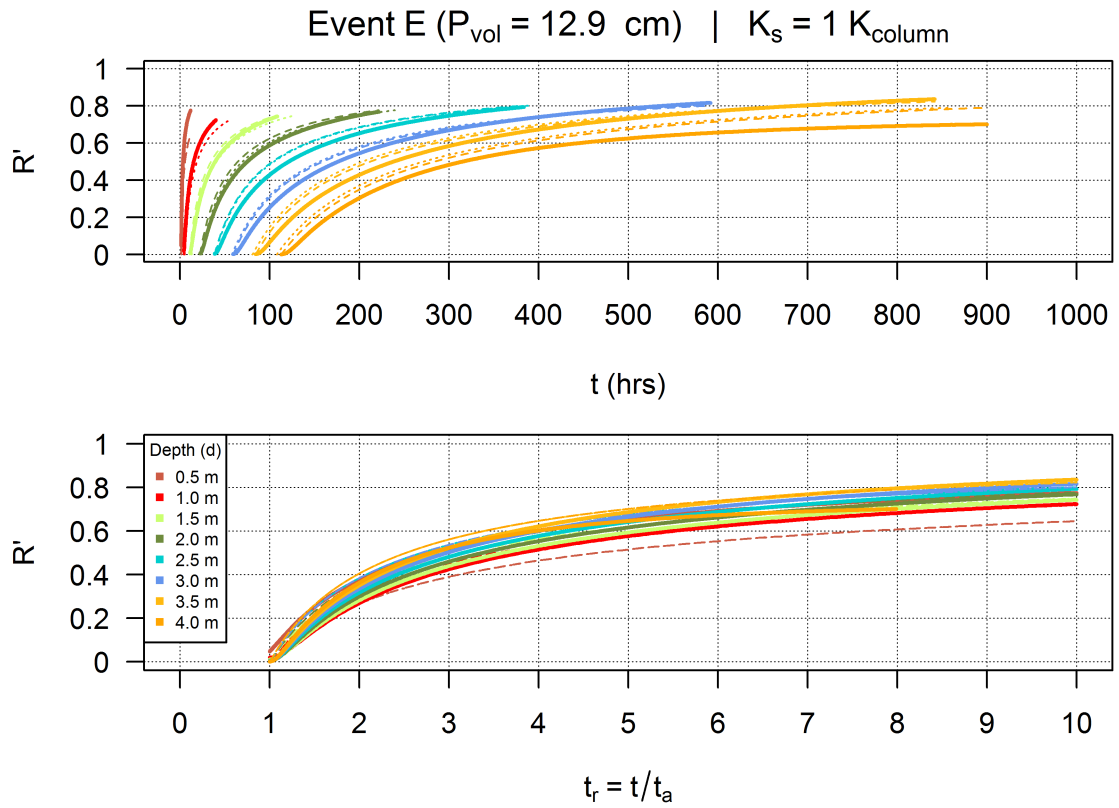
Figure 3.22: Model estimated relative recharge (R') at different depths for Event E from simulation set 7. (R') is plotted against time, t (top) and relative time, t_r (bottom). $K_s = 1$ K_{column} as listed in Table 3.1.
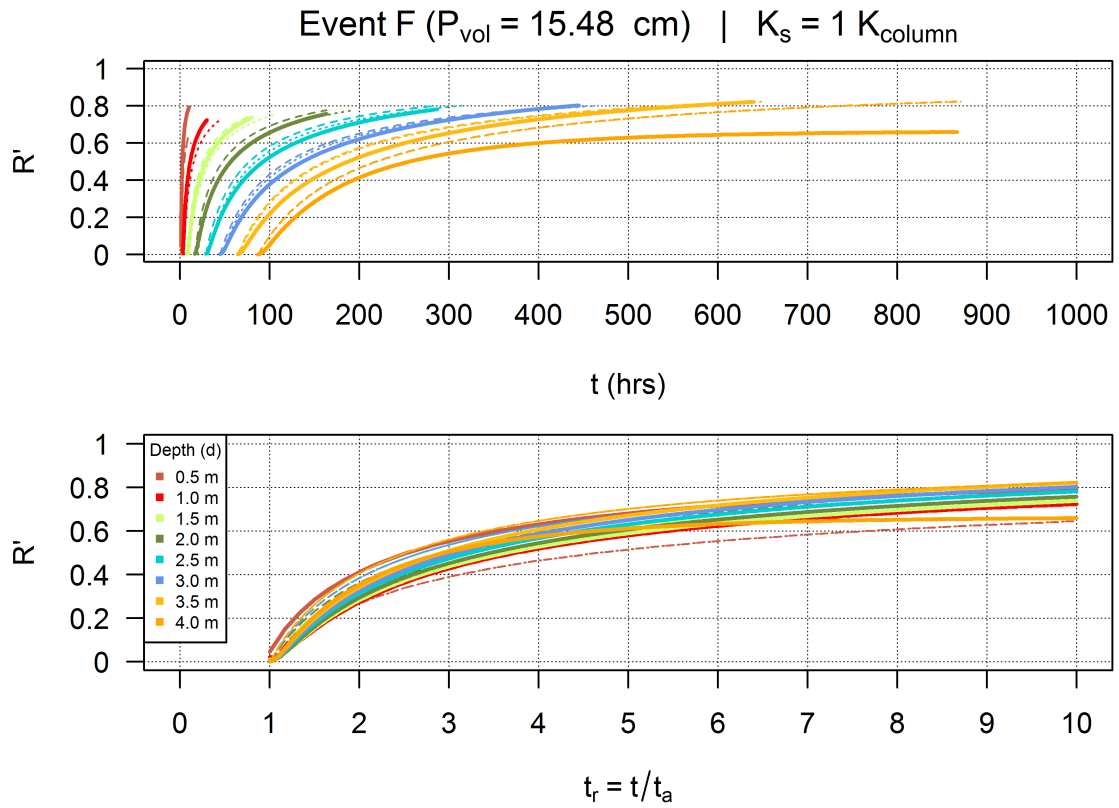
Figure 3.23: Model estimated relative recharge (R') at different depths for Event F from simulation set 7. (R') is plotted against time, t (top) and relative time, t_r (bottom). $K_s = 1 \ K_{column}$ as listed in Table 3.1.

$$t_r = t/t_a \tag{3.18}$$

where t_r is the relative time, t is the model time, t_a is the time of arrival at the given depth.

The relative recharge for different depths was plotted against the relative time as shown in Figures 3.18 through 3.23. The solid lines show the simulated recharge. The dashed lines show recharge calculated predicted by the model based on modeled t_a. The dotted lines show the predicted recharge based on t_a predicted by the t_a model. A set of curves of the form given by Equation 3.19 were fitted for each depth.

$$R_d' = 1 - 1/t_r^\gamma \tag{3.19}$$

where γ is the power that fits the R_d' curve to the equation 3.17 for the estimation of R' for depth d.

The power (γ) in Equation 3.19 for relative recharge was found to be a function of the depth at which the recharge is calculated. Equation 3.20 relates the γ to the depth (d) at which the relative recharge is estimated.

$$\gamma = 0.45 + 0.1\ d \tag{3.20}$$

The model described in Section 3.3.1 can be used to estimate the timing of wetting front arrival at a given depth. After calculating the arrival time, the progression of relative recharge at that depth can be estimated by the model described here.The error in the prediction of the relative recharge is discussed in Chapter 4. The range of applicability of the proposed equations and limitations are also discussed in Chapter 4.

Chapter 4 Results and Discussions

The models developed in Chapter 3 were tested with a set of new rainfall events and saturated hydraulic conductivities that were not previously used in the model development. The rainfall events used for model validation are given in Table 4.1. The models were tested with 11 different K_s values with 6 rainfall events ranging from 1.2 inches to 15.2 inches for each K_s value.

4.1 Validation of Model t_a: Arrival Time

The proposed models for the arrival time at different depths were tested with the varying conditions specified in Table 4.1. The pulse volume (P_{vol}) for each rainfall event was calculated by multiplying the intensity (cm/hr) given in Table 4.1 to 60 minutes. To calculate the excess moisture (θ'), P_{vol} was divided by the depth (d) at which the wetting front arrival time has to be calculated according to Equation 3.12 given in Chapter 3. For the purpose of model validation, the time of arrival was calculated for 40 depths (d) at 10 cm intervals starting from 10 cm below land surface through 400 cm below land surface. The calculated excess moisture (θ') was then used to predict the timing of recharge by using Equations 3.14 and 3.15 as given in Chapter 3. The timing of recharge can be calculated by using Equation 4.1.

$$t_a = t_n \frac{d}{Ks} \tag{4.1}$$
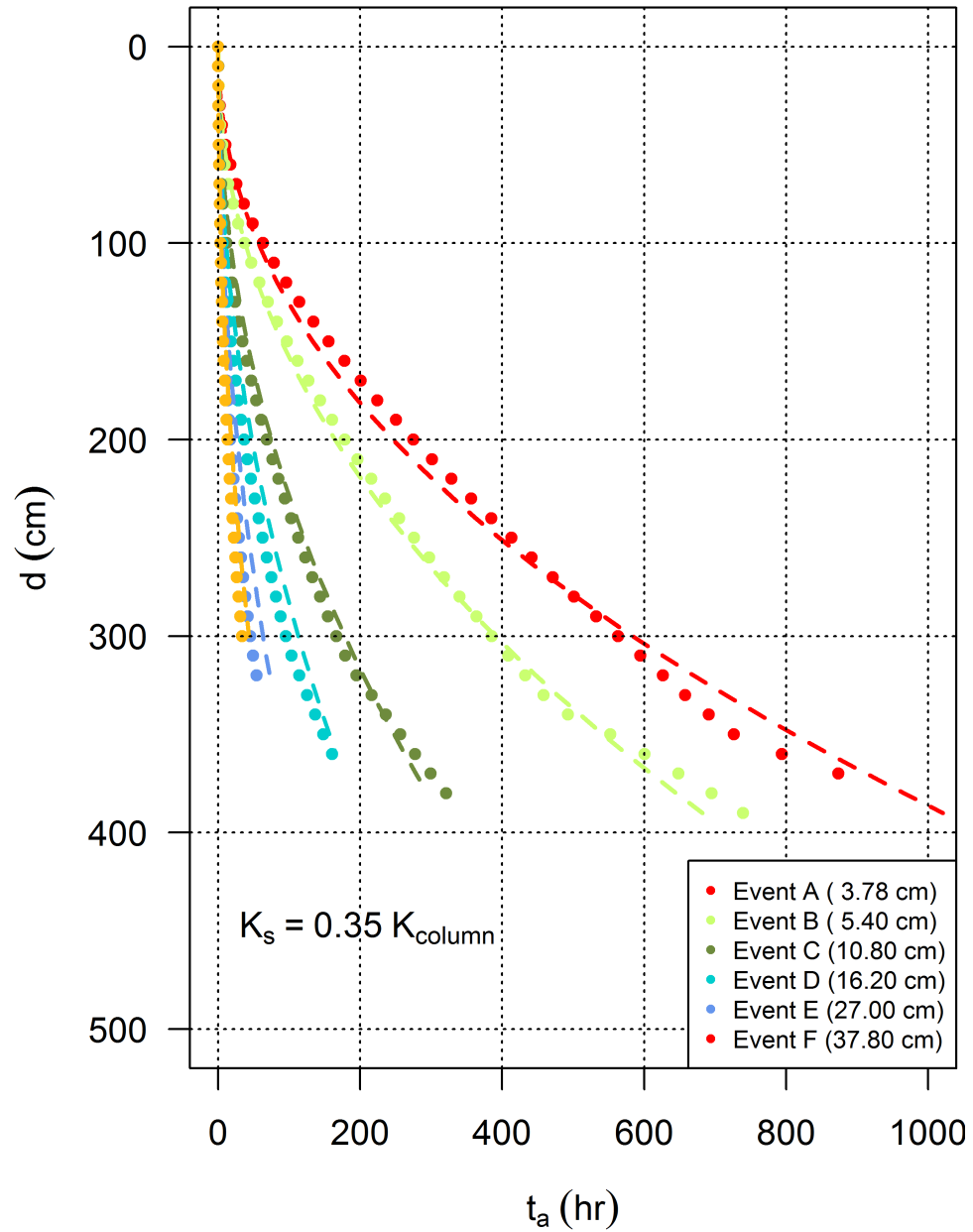
Figure 4.1: Time of arrival (t_a) of the wetting front at different depths (*dashes* – Proposed Model, *points* – HYDRUS simulation). Six events (A through F) from simulation case 3 (from Table 4.1) are shown.

Table 4.1: Applied rainfall intensities and Ks multiplier for model validation. Six different intensities applied for each Ks value.

Simulation Set	1	2	3	4	5	6	7	8	9	10	11
Ks multiplier[1]	0.20	0.25	0.35	0.45	0.55	0.85	1.25	1.55	3.00	7.00	9.00
Event A[2]	6.2	3.9	3.8	3.5	4.3	3.9	9.7	12.0	9.3	5.4	2.8
Event B	9.3	7.7	5.4	4.9	6.4	6.6	14.5	18.0	13.9	10.8	7.0
Event C	15.5	11.6	10.8	7.0	8.5	9.2	19.4	24.0	23.2	16.3	13.9
Event D	21.7	19.4	16.3	13.9	10.6	13.2	24.2	30.0	32.5	21.7	20.9
Event E	31.0	27.1	27.1	20.9	12.8	26.3	29.0	36.0	37.2	32.5	27.9
Event F	46.4	38.7	37.9	34.8	17.0	39.5	38.7	48.0	46.4	54.2	34.8

[1] This factor was multiplied with Ks of soil column to get Ks for this simulation
[2] Events intensities in cm/hr

The normalized root mean square errors ($nRMSE$) (Equation 4.7) for the predicted time of arrival are given in Table 4.2 for all the simulation cases listed in Table 4.1. The $nRMSE$ of the predicted time was less than 15 percent for 75 percent (3rd Quartile) of the tested recharge cases and less than 22 percent for the worst case prediction, which corresponds to an extremely high value of K_s and a very high volume of applied event (Table 4.2). The estimated time of arrival (dashed line) plotted against the simulated time of arrival (points) is shown in Figure 4.1. Using these calculations of the time of arrival (t_a) at the specified depths, the progression of recharge at these depths was calculated as described in Section 4.2. The errors in the time of arrival result in a slight shift in the onset of modeled recharge (described in Section 4.2).

$$t_r = t/t_a \tag{4.2}$$

$$R_d' = 1 - 1/t_r^{\gamma} \tag{4.3}$$

$$\gamma = 0.45 + 0.1 \; d \tag{4.4}$$

Table 4.2: Normalized root mean square errors (percentage) in the prediction of timing of arrival (t_a) of the wetting front. The depth (d) for t_a ranged from 10 cm to 400 cm.

Simulation Set	1	2	3	4	5	6	7	8	9	10	11
Event A	3.6	4.4	3.4	5.4	3.3	3	6.6	7.8	5.9	4.5	3.4
Event B	5.4	4.5	2.2	2.7	2.2	1.3	2.1	2.2	1.7	3.7	2.8
Event C	4.7	3.8	2.7	1.1	0.9	1.6	6.2	7.5	10.4	9.1	11
Event D	9.6	8.7	6.2	5.8	1.6	5.8	12	13.2	16.2	12.1	15
Event E	14.4	17.1	18	13.5	3.7	21.2	16.6	16.3	18.3	14.9	16.2
Event F	6.2	6.4	13.7	20.3	8.1	21.5	21.1	13.5	17.4	21.8	18.4

$$R_d' = 1 - \frac{1}{\left[\frac{t}{t_n \frac{d}{Ks}} \right]^{(0.45 + 0.1\ d)}} \tag{4.5}$$

$$RMSE = \sqrt{\frac{\sum_1^n (observed - modeled)^2}{n}} \tag{4.6}$$

where n is total number of values from *observed* and *modeled*, the two sets being used to calculated the error.

$$nRMSE = 100 \ \frac{RMSE}{Observed_{max} - Observed_{min}} \tag{4.7}$$

where $Observed_{max}$ and $Observed_{min}$ are the maximum and minimum value in the *observed* set from Equation 4.6.

4.2 Validation of Model R': Progression of Recharge

The arrival of the recharge at a specified depth was calculated as described in Section 4.1. After calculating the arrival time, the recharge was calculated using the model developed and described in Section 3.3.2 (R' model). Equation 4.5 is the proposed equation to calculate the time accumulation of groundwater recharge.

The root mean square error (RMSE) (Equation 4.6) in the estimation of relative recharge is given in Table 4.3 for all of the modeled cases. RMSE has been used instead of

Table 4.3: Root mean square errors (percentage) in the prediction of the relative recharge (R'). The intensity of the applied events is given in Table 4.1.

Simulation Set	1	2	3	4	5	6	7	8	9	10	11
Event A	4.56	4.86	4.55	4.47	3.93	3.82	3.96	3.20	3.52	5.23	3.50
Event B	4.09	4.16	4.02	4.16	3.42	3.17	3.55	4.22	4.34	4.56	4.37
Event C	3.25	3.68	3.60	3.60	3.06	3.39	4.15	4.38	4.44	4.30	6.18
Event D	3.00	3.12	3.24	3.18	2.88	4.26	4.65	3.71	3.98	4.65	5.46
Event E	–	2.79	3.24	3.67	2.93	4.27	4.42	3.53	4.58	1.30	7.38
Event F	–	–	–	3.09	3.18	3.17	3.29	1.21	1.93	14.46	5.95

the normalized RMSE for error analysis since the predicted recharge is already normalized between 0 and 1. The RMSE of the predicted relative recharge was found to be less that 4 percent for 75 percent of the cases (3rd Quartile). The highest error in estimation of R' was found to be 14 percent, which corresponds to the extreme case of a very high K_s value with a large applied pulse volume. Figure 4.2 shows the model estimated relative recharge (dotted) calculated from estimated time of arrival against the recharge estimated based on the simulated time of arrival (dashed). The solid line in Figure 4.2 shows the simulated relative recharge. As can be seen in Figure 4.2, the recharge estimated from the proposed model starts early or later than the simulated recharge because of the error in estimation of the time of arrival at that depth. This error in estimation of arrival time may delay or advance the predicted onset of recharge.

4.3 Comparison with Field Data

The arrival time of the wetting front corresponding to the rainfall events from the field is given in Section 2.2.2. The proposed model was used to calculated the wetting front arrival time of different applied pulse volumes (P_{vol}) and compared to the t_a observed in the field (Figure 4.3). The effective P_{vol} was calculated after accounting for the volume required to reach the wet equilibrium. This P_{vol} was then 1used to calculate θ' for predicting the t_a using proposed equations.
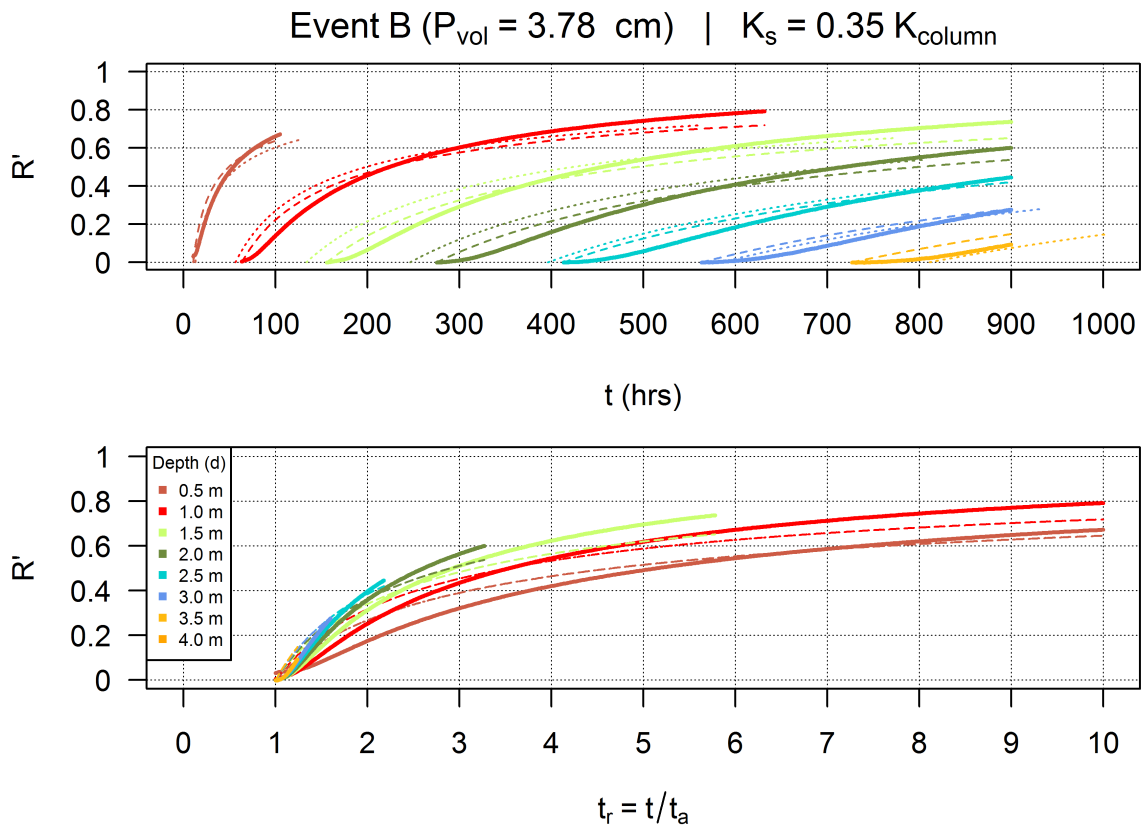
Figure 4.2: Model estimated relative recharge (R') of the wetting front at different depths. Event B from simulation set 3 (from Table 4.1) is shown.
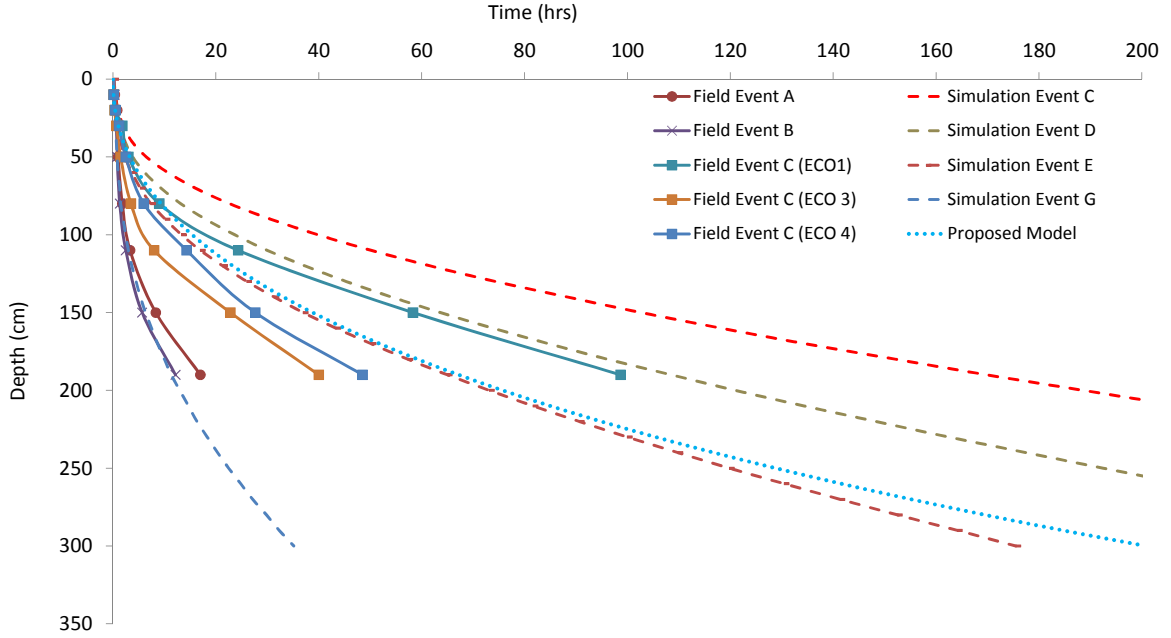
Figure 4.3: Wetting front arrival time (t_a) for rainfall events in the field compared with t_a calculated using the proposed model. Events C, D, E, and G from simulation set 5 (from Table 4.1) are shown for comparison.

4.4 Discussion

The root mean square error in prediction of the time of arrival was found to be less than 10 hours for 75 percent (3rd Quartile) of the tested recharge cases. The proposed model was found to predict the time of arrival (onset of recharge) with reasonable accuracy for the entirely new dataset. Also, for the validation dataset, the root mean square error in the prediction of relative recharge was found to be less than 4 percent for 75 percent (3rd Quartile) of the tested recharge cases. Results from the validation runs indicate that the progression of relative recharge can be estimated by the proposed model with reasonable accuracy.

The observed time of arrival (t_a) for the observed rainfall events in the field was compared to the t_a predicted using the proposed models. As shown in Figure 4.3, the

model can be used to predict t_a for field soil conditions, by calculating the effective P_{vol} after accounting for the volume required for reaching the wet equilibrium.

4.5   Assumptions

The proposed models described here assume that once the wetting front reaches the capillary zone, it results in an instant recharge to the water table verified by field, lab, and HYDRUS testing. Therefore, the depth considered for timing to recharge predictions should be based on depth to capillary zone, rather than depth to water table.

It must be understood that the validation was for a specific retention curve within the range of model calibration. The development runs (calibration) were based on a range of water retention curves as shown in Figure 3.17. The effect of using different water retention curves is discussed in Section 3.3.1.

Chapter 5 Summary and Conclusions

The recharge estimated using the proposed model was found to be a function of the depth at which the recharge is calculated, after the onset of recharge. The onset of recharge (t_a) was found to be strong function of the excess moisture above equilibrium (θ'), which is directly dependent on the volume of applied pulse (P_{vol}). As expected, higher applied volume resulted in shorter time of arrival. The predictive capabilities of the proposed model were not sensitive to the volume since the model is based on normalized pulse rather than the absolute volume. Arrival time, t_a, was also a weak function of the K_s which is expected since the effect of K_s was already weakened by normalizing the arrival time by dividing it by K_s in Equation 3.10.

The focus of this dissertation was to study the time scale of recharge to develop a simple model that predicts the onset of groundwater recharge at a specified depth and predicts the progression of groundwater recharge. For a preliminary analysis of the time scale of recharge, high resolution soil moisture data from the field study were used to investigate the propagation of the soil moisture wetting front following isolated rainfall events. However, the field study environment provided limited flexibility to study the time scale of recharge because of the lack of control over the evapotranspiration (ET) processes, rainfall intensities, complex heterogeneous layering of soils, difficulty in installing tensiometer and soil moisture sensors. This provided motivation for the construction of a laboratory soil column that was used to study soil moisture wetting front under controlled conditions to understand the time scale of recharge.

The laboratory soil column provided an environment with control over the volume and intensity of the applied 'rainfall' events with no effect of ET or root water uptake. However, the height of the laboratory soil column (170 cm) limited the observed wetting front propagation to only about 100 cm above the capillary zone. To overcome this limitation, a computer model was calibrated to represent the laboratory soil column using the observed high resolution soil moisture, water table and tensiometer data from the soil column in the laboratory. The computer model used the soil hydraulic conductivity determined by a constant head permeability test on the laboratory soil column. This computer model was then extended in length to simulate deeper water table conditions and study wetting front propagation corresponding to a variety of applied 'rainfall' pulses and a variety of soil hydraulic parameters.

The data generated from the simulation of a wide range of applied rainfall pulses and soil hydraulic conductivities were analyzed for the time scale of propagation of the wetting front and the progression of recharge. A set of simple equations was proposed to model the propagation of the wetting front representing the onset of groundwater recharge at a given depth. Another set of equations was proposed to model the progression of groundwater recharge after the onset of recharge. This dissertation provides a set of simple equations to model the time scale of the onset recharge for a given depth and the progression of recharge following its onset. The time of arrival of the wetting front at a given depth (indicating the onset of recharge) can be calculated by the proposed model with a reasonable accuracy (errors less that 14%) for a given water retention curve. The dependence of the proposed models on the water retention curve is studied briefly in this dissertation and should provide a basis for a proposed future study. Also, the proposed methodology can be used to study the effects of the root water uptake in evapotranspiration environment and the proposed models can be extended to include the root water uptake zone (Figure 5.1). The effects of root water uptake and evapotranspiration can be studied in future to explain the apparent delay or elimination of recharge from root water uptake.
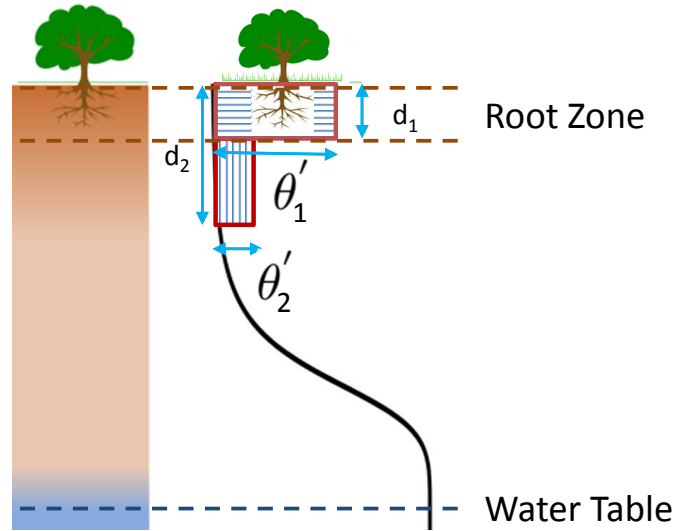
Figure 5.1: Schematic diagram showing the root zone affecting θ' because of root water uptake. Calculation of P_{vol} under root water uptake environment is suggested as future work.

The simplifying models developed here are valid for negligible ET and/or the region below the root zone. Further investigation of the effects of ET and a wider range of soil parameters (other than typical Florida fine sands) has been proposed as future work.

This dissertation provides a framework for better representation of groundwater recharge in coupled and integrated hydrological models. The proposed models are simple, computationally inexpensive and require a few easily obtainable soil hydraulic parameters. This approach should be useful for representing and calculating groundwater recharge when the soil data available for modeling groundwater recharge is limited. The approach is computationally inexpensive yet relatively accurate.

This dissertation contributes to the representation of complex hydrological processes using simple models to make the modeling and management of water resources easier and practical by using readily available data. This study focused on the time scale of the complex recharge process for typical water retention curves. The methodology described in this dissertation can tested to extend the concept for different root water uptake environments for studying the effect of evapotranspiration on the calculation of P_{vol} (Figure 5.1). It can

also be applied to study the effect of different soils by testing it on soils with different hydrological parameters representing a wider range of water retention curves.

List of References

ASTM (2012). Standard test methods for laboratory compaction characteristics of soil using standard effort. In *D 698-12*. ASTM, Philadelphia, PA.

Barlow, P., DeSimone, L., and Moench, A. (2000). Aquifer response to stream-stage and recharge variations. ii. convolution method and applications. *Journal of Hydrology*, 230(3):211–229.

CMHAS (2011). Measurement of evapotranspiration, recharge, and runoff in transitional water table environments. Technical report, Department of Civil and Environmental Engineering, University of South Florida, Tampa, Florida.

DHI (2004). *MIKE SHE: An Integrated Hydrological Modeling System*. Hørsholm, Denmark.

Diodato, D. M. (2000). Software spotlight. *Ground Water*, 38(1):10–11.

Freeze, R. A. and Cherry, J. (1979). *Groundwater*. Prentice-Hall, Englewood Cliffs, NJ.

Gerhart, J. M. (1986). Ground-water recharge and its effects on nitrate concentration beneath a manured field site in pennsylvania. *Ground Water*, 24(4):483–489.

Graham, D. N. and Butts, M. B. (2005). Flexible, integrated watershed modelling with mike she. In Singh, V. and Frevert, D., editors, *Watershed Models*, volume 0849336090, pages 245–272. CRC Press.

Hall, D. W. and Risser, D. W. (1993). Effects of agricultural nutrient management on nitrogen fate and transport in lancaster county pennsylvania1. *JAWRA Journal of the American Water Resources Association*, 29(1):55–76.

Harter, T. and Hopmans, J. W. (2004). Role of vadose zone flow processes in regional scale hydrology: review, opportunities and challenges. In Feddes, R., de Rooij, G., and van Dam, J., editors, *Unsaturated zone modeling: Progress, applications, and challenges*. Kluwer Academic Publishers, Boston, MA.

Hernandez, T., Nachabe, M., Ross, M., and Obeysekera, J. (2003). Modeling Runoff from Variable Source in Humid, Shallow Water Table Environments. *Journal of the American Water Resources Association*, 39:75–85.

Hughes, J. D. and Liu, J. (2008). MIKE SHE: Software for integrated surface water/ground water modeling. *Ground Water*, 46(6):797–802.

Illangasekare, T. and Prucha, R. (2001). Dhi-water and environment, 2001. *MIKE SHE Code Verification and Validation for RFETS Site-Wide Water Balance Model.*

Jayatilaka, C. and Gillham, R. (1996). A deterministic-empirical model of the effect of the capillary fringe on near-stream area runoff 1. description of the model. *Journal of Hydrology*, 184(3):299–315.

Lee, T. (1996). Hydrogeologic controls on the groundwater interactions with an acidic lake in karst terrain, lake barco, florida. *Water Resources Research*, 32(4):831–844.

Markstrom, S. L., Niswonger, R. G., Regan, R. S., Prudic, D. E., and Barlow, P. M. (2008). *GSFLOW, Coupled Ground-Water and Surface-Water Flow Model Based on the Integration of the Precipitation-Runoff Modeling System (PRMS) and the Modular Ground-Water Flow Model (MODFLOW-2005).* US Department of the Interior, US Geological Survey.

Mualem, Y. (1976). A new model for predicting the hydraulic conductivity of unsaturated porous media. *Water resources research*, 12(3):513–522.

Nachabe, M. H. (2002). Analytical expressions for transient specific yield and shallow water table drainage. *Water Resources Research*, 38(10):11–1.

Rahgozar, M., Shah, N., and Ross, M. (2007). Estimation of evapotranspiration and water budget components using continuous soil moisture and water table monitoring. In *World Environmental and Water Resources Congress 2007@ sRestoring Our Natural Habitat*, pages 1–23. ASCE.

Rahgozar, M., Shah, N., and Ross, M. (2012). Estimation of evapotranspiration and water budget components using concurrent soil moisture and water table monitoring. *ISRN Soil Science*, 2012:15.

Rahgozar, M. S. (2006). *Estimation of evapotranspiration using continuous soil moisture measurements.* Ph.d. dissertation, University of South Florida, Tampa.

Richards, K., Coxon, C. E., and Ryan, M. (2005). Unsaturated zone travel time to groundwater on a vulnerable site. *Irish Geography*, 38(1):57–71.

Richards, L. A. (1931). Capillary conduction of liquids through porous mediums. *Physics*, 1(5):318–333.

Ross, M., Geurink, J., Aly, A., Tara, P., Trout, K., and Jobes, T. (2004). Integrated hydrologic model (ihm), volume i: theory manual. *Tampa Bay Water and Southwest Florida Water Management District.*

Said, A., Nachabe, M., Ross, M., and Vomacka, J. (2005). Methodology for estimating specific yield in shallow water environment using continuous soil moisture data. *Journal of irrigation and drainage engineering*, 131(6):533–538.

Scanlon, B., Healy, R., and Cook, P. (2002). Choosing appropriate techniques for quantifying groundwater recharge. *Hydrogeology Journal*, 10(1):18–39.

SENTEK (2003). *Access Tube Installation Guide.* Adelaide, South Australia, version 1.0 edition.

Shah, N. and Ross, M. (2009). Variability in specific yield under shallow water table conditions. *Journal of Hydrologic Engineering*, 14(12):1290–1298.

Šimůnek, J., van Genuchten, M. T., and Šejna, M. (2005). The HYDRUS-1D software package for simulating the one-dimensional movement of water, heat, and multiple solutes in variably-saturated media, version 3.0. *Manual of HYDRUS Software Series 1, Department of Environmental Sciences, Univ. California Riverside, Riverside, Calif.*

Stephens, D. B. and Rehfeldt, K. R. (1985). Evaluation of closed-form analytical models to calculate conductivity in a fine sand1. *Soil Sci. Soc. Am. J.*, 49(1):12–19.

Sumner, D. M. (1996). Evapotranspiration from successional vegetation in a deforested area of the Lake Wales Ridge, Florida. U.S. Geological Survey Water-Resources Investigations Report 96-4244, USGS.

Swancar, A. and Lee, T. M. (2003). Effects of Recharge, Upper Floridan Aquifer Heads, and Time Scale on Simulated Ground-water Exchange with Lake Starr, a Seepage Lake in Central Florida. U.S. Geological Survey Water-Resources Investigations Report 02-4295, USGS.

Todd, D. K. (1959). *Groundwater hydrology.* J. Willey and Sons.

Trout, K. and Ross, M. (2006). Estimating evapotranspiration in urban environments. In *Urban groundwater management and sustainability*, pages 157–168. Springer.

van Genuchten, M. T. (1980). A closed-form equation for predicting the hydraulic conductivity of unsaturated soils. *Soil Science Society of America Journal*, 8:892–898.

Virdi, M. L., Lee, T. M., Swancar, A., and Niswonger, R. G. (2012). Simulating the effect of climate extremes on groundwater flow through a lakebed. *Ground Water*.

Ward, A., Wells, L. G., and Phillips, R. E. (1983). Characterizing unsaturated hydraulic conductivity of western kentucky surface mine spoils and soils1. *Soil Sci. Soc. Am. J.*, 47(5):847–854.

Appendices

Appendix A Glossary of Terms

Antecedent Moisture Condition : Relatively dry or wet soil moisture conditions preceding a rainfall event.

Capillary Zone : The zone extending immediately above the water table which holds moisture, drawn from the water table because of capillary action.

Dry Equilibrium : A state of pseudo-static equilibrium drier than the equilibrium, which is stable over practical time scales. Removal of water from this equilibrium state will eventually result in a drop in water table.

Effective Saturation : A representation of normalized soil moisture content, used in the *van Genutchen model* for water retention curve.

Hydraulic Conductivity : A soil property that is a measure of its ability to conduct water across a *Hydraulic gradient.*

Hydraulic Gradient : A vector gradient between hydraulic heads along the flow direction.

Matric Suction : Negative pressure exerted by dry soil matrix because of pore-air pressure and pore-water pressure, attributed mainly to capillary action.

Root Water Uptake : Water extracted by the roots of plants from the soil.

Soil Moisture Content : Volume of water per unit volume of soil, also called *Soil water content.*

Soil Moisture Profile : A profile showing the vertical distribution of *Soil moisture content* in a one dimensional column of soil.

Unsaturated Zone : The zone extending from the water table to the land surface, also called *Variably saturated zone*, *Unsaturated zone*, or *Vadose zone.*

Water Retention Curve : A relationship between the soil moisture content and soil matric suction head.

Wet Equilibrium : A state of pseudo-static equilibrium wetter than the equilibrium, which is stable over practical time scale of recharge. Addition of water to this equilibrium state will eventually result in a rise in water table.

Appendix B Notations

Symbol	Represents
c_1	Coefficient for t_a equation
c_2	Coefficient for λ equation
t_n	Dimensionless wetting front arrival time
Θ	Effective saturation
P_{vol}	Effective volume of applied pulse
ψ	Matric suction
n	Pore-index parameter for VGM model
γ	Power used in proposed R' equation
λ	Power used in proposed t_a equation
R'	Relative recharge
θ_r	Residual soil water content
K_s	Saturated hydraulic conductivity of soil
θ_s	Saturated soil water content
$P_{applied}$	Volume of applied pulse
θ	Volumetric soil moisture content
t_a	Wetting font arrival time

Appendix C Integration of van Genutchen WRC (Python Code)

```python
'''
Program to integrate van Genutchen (1980) Water Retention Curve
to calculate equilibrium water table elevation following addition
of a know Volume of water to a 1-Dimensional soil column

Created on Feb 2, 2013
@author: Makhan Virdi
'''
import mpmath
mpmath.dps = 25; mpmath.pretty = True

ThetaS = 0.36
ThetaR = 0.045
alpha = 0.018288
n = 6.378
m= 1-(1/n)
d1 = 0. # WT1
d2 = 1000. # WT2

power1 = -pow((alpha*d1),n)
power2 = -pow((alpha*d2),n)

# Evaluate Gauss' Hypergeometric function 2F1
F1 = mpmath.hyp2f1(m,1/n,1+1/n,power1)
F2 = mpmath.hyp2f1(m,(1/n),(1+(1/n)),power2)

F_d1 = d1*( (ThetaS-ThetaR)*F1 +ThetaR   )
F_d2 = d2*( (ThetaS-ThetaR)*F2 +ThetaR   )
F = F_d2 - F_d1

Fvol = []

configs = list(mpmath.arange(0.0, 1000.0, 0.01))
for WTconfig in configs:
    power2 = -pow((alpha*WTconfig),n)
    F2 = mpmath.hyp2f1(m,(1/n),(1+(1/n)),power2)
    F_WTconfig = WTconfig*( (ThetaS-ThetaR)*F2 +ThetaR   )
    F = F_WTconfig - F_d1
    Fvol.append(F)

#Write   configs (Serial Number), DTWT, and Wvolumes
with open('TSM-WT.txt', 'w') as f:
    for f1, f2 in zip(configs, Fvol):
        print >> f, f1, f2
```

VGMintegration.py

Appendix D Calculation of Normalized Recharge (R Code)

```r
# Name of the folder for output files
AnalysisFolder <- "3_WRC_d_Ks_All"
library(minpack.lm)

na.pad <- function(x,len){
  x[1:len]
}

makePaddedDataFrame <- function(l,...){
  maxlen <- max(sapply(l,length))
  data.frame(lapply(l,na.pad,len=maxlen),...)
}

specify_decimal <- function(x, k) format(round(x, k), nsmall=k)

RE_WRITE_FILES <- 1 # Flag to rewrite files
KsFactorVector   <- c(0.12, 0.2,      0.3,     0.4,    0.5,     0.7,      1,
    1.5, 2, 5, 10)
KsVector         <- c(0.02,0.0344, 0.0516, 0.0688, 0.086, 0.1204, 0.172,
    0.258, 0.344, 0.86, 1.72)
factorfile <- paste("C:\\Users\\mvirdi\\Documents\\Work\\
    ExcelAnalysisVadose\\WaterTable5m\\",AnalysisFolder,"\\Y_SetsFactors
    .csv",sep="")
SetsFactors = read.csv(file=factorfile, na.strings = "#N/A", header=TRUE
    ,sep=",", skip=0)

set2rains <- (length(SetsFactors$sets) - 1)  #7 Events ('a' through 'g')
RechargeDepths <- seq(50,400,50) # cm
t_ratio_max <- 10 # max of t/ta to cut-off analysis
TotalKsRuns <- length(KsVector)
powerheader <- c("KsFactor", "Ks", "PulseFactor", "Event","PulseVol",
    paste("Power", RechargeDepths/100,"m",sep=""), paste("P",
    RechargeDepths/100,"m",sep=""))
superpowers_misc_cols <- 5 # number of cols with misc data viz. |
    KsFactor | Ks | PulseFactor | Event | PulseVol |
superpowers <- as.data.frame(matrix(nrow = set2rains*TotalKsRuns, ncol =
     length(powerheader)))
colnames(superpowers) <- powerheader

superpowers$KsFactor <- rep(KsFactorVector, each=set2rains)
superpowers$Ks <- rep(KsVector, each=set2rains)
superpowers$PulseFactor <- as.vector(as.matrix(SetsFactors[2:(set2rains
    +1),2:(TotalKsRuns+1)]))
superpowers$Event <- rep(paste("Event ", LETTERS[1:set2rains],sep=""),
    TotalKsRuns)
superpowers$PulseVol <- superpowers$Ks*superpowers$PulseFactor*60
```

```
37  for (depth_seq in 1:length(RechargeDepths))
      superpowers[,superpowers_misc_cols+length(RechargeDepths)+depth_seq]
        <- superpowers$PulseVol/RechargeDepths[depth_seq]
39
    for (Ks.this in seq(1,TotalKsRuns))
41    {
      KsFactor <- KsFactorVector[Ks.this]
43    KsCase <- paste("Ks",KsFactor,sep="")   #Folder name

45    KsFactorFile <- KsFactor
      Ks <- KsVector[Ks.this]
47
      PulseFactorColumn <- Ks.this+1 # refer to "SetFactors" on "Index and
        Notes.xlsx"
49    # Read Input Data: MODELING DIRECTORY
      WorkingDir <- "C:\\Users\\mvirdi\\Documents\\Work\\Hydrus1D\\Projects
        \\WaterTableRecharge\\WRC_t_10_autoKs_factor7pulse"
51    InputDirectory <- paste(WorkingDir,"\\",KsCase,sep="")
      setwd(InputDirectory)
53    obsfile <- list.files(pattern=paste("OBS_NODE.OUT.",KsFactorFile,".*.*
        ",sep="")) #csv"

55    # 'sets' with 'h' for each event for all times
                  # 'time ' > 90000
      hsets <- c(paste("h1"),paste("h2",letters[1:set2rains],sep=""))
57    for (i in 1:length(obsfile)) {
        obsnodefile <- obsfile[i]
59      mdata <- read.table(file=obsnodefile, header=FALSE, skip=11, comment
        .char="e")   #comment.char="e" correspond to "end" in last line6

61      timecol <- 1
        hcol <- c(timecol, seq(from = 2, to = 167, by = 3)) # DO we need
      first column (time) ????
63      mh <- (subset(mdata, select = hcol))

65      sub_mh <- mh #subset(mh, mh$V1 >= 90000)
        assign(hsets[i], sub_mh)
67
        write_h <- paste("C:\\Users\\mvirdi\\Documents\\Work\\
        ExcelAnalysisVadose\\WaterTable5m\\",AnalysisFolder,"\\h\\", hsets[i
        ],"_",KsFactorFile,"Ks.csv",sep="")
69
        if (RE_WRITE_FILES ==1 )
71        write.csv(eval(as.name(hsets[i])), file = write_h, row.names =
      FALSE)
      }
73    # 'sets' with 'theta' for each event for 'time ' > 90000 min
```

Appendix D (continued)

```r
     sets <- c(paste("theta1"),paste("theta2",letters[1:set2rains],sep=""))
75   for (i in 1:length(obsfile)) {
       obsnodefile <- obsfile[i]
77     mdata <- read.table(file=obsnodefile, header=FALSE, skip=11, comment
       .char="e")

79     timecol <- 1
       smcol <- c(timecol, seq(from = 3, to = 168, by = 3))
81     mtheta <- (subset(mdata, select = smcol))

83     sub_mtheta <- subset(mtheta, mtheta$V1 >= 90000)
       assign(sets[i], sub_mtheta)
85
       write_theta <- paste("C:\\Users\\mvirdi\\Documents\\Work\\
       ExcelAnalysisVadose\\WaterTable5m\\",AnalysisFolder,"\\theta\\",
       sets[i],"_",KsFactorFile,"Ks.csv",sep="")
87
       if (RE_WRITE_FILES ==1 )
89       write.csv(eval(as.name(sets[i])), file = write_theta, row.names =
       FALSE)
     }
91
     del_theta <- c(paste("del_theta1"),paste("del_theta2",letters[1:
       set2rains],sep=""))
93   for (i in 1:length(obsfile)) {
       off_sets <- ( eval(as.name(sets[i])) - eval(as.name(sets[1])) )
95     off_sets[1] <- theta1[1]-90000
       assign(del_theta[i], off_sets)
97
       write_del_theta <- paste("C:\\Users\\mvirdi\\Documents\\Work\\
       ExcelAnalysisVadose\\WaterTable5m\\",AnalysisFolder,"\\del_theta\\",
       sets[i],"_",KsFactorFile,"Ks.csv",sep="")
99     if (RE_WRITE_FILES ==1 )
         write.csv(eval(as.name(del_theta[i])), file = write_del_theta, row
       .names = FALSE)
101  }
     # Find Time of Arrival at 0.5 m intervals: mtimes
103  times <- c(paste("depth"),paste("times2",letters[1:set2rains],sep=""))
     assign( times[1], c(seq(0,500,10), seq(600,1000,100)) )
105
     for (sensor in 2:length(times)) { #for each EVENT
107    assign( times[sensor], NULL)
       for (col in 2:length(eval(as.name(del_theta[sensor])))) {
109      t_rise <- min(eval(as.name(del_theta[sensor]))$V1[which(eval(as.
       name(del_theta[sensor]))[,col] > 0.001)]) # old threshold = 0.001
         assign( times[sensor] , c(eval(as.name(times[sensor])), t_rise) )
111    }
```

```r
      }
113   times <- data.frame(depth, times2a,times2b,times2c,times2d,times2e,
        times2f,times2g)
      is.na(times) <- do.call(cbind,lapply(times, is.infinite)) # convert '
        Inf' to 'NA'
115   mtimes <- times[depth %in% RechargeDepths,]
      writetimes <- paste("C:\\Users\\mvirdi\\Documents\\Work\\
        ExcelAnalysisVadose\\WaterTable5m\\",AnalysisFolder,"\\times\\", "
        times_", KsFactorFile,"Ks.csv",sep="")
117   if (RE_WRITE_FILES ==1 )
        write.csv(times, file = writetimes, row.names = FALSE)
119
      m1 <- mtimes[-1,]
121   m2 <- mtimes[-nrow(mtimes),]
      diff_m <- m1-m2
123   diff_m <- rbind(rep(1,length(times)),diff_m)
      diff_m$depth <- RechargeDepths
125   diff_m$times2a[diff_m$times2a < 0] <- 0
      diff_m$times2a[diff_m$times2a > 0] <- 1
127   diff_m$times2b[diff_m$times2b < 0] <- 0
      diff_m$times2b[diff_m$times2b > 0] <- 1
129   diff_m$times2c[diff_m$times2c < 0] <- 0
      diff_m$times2c[diff_m$times2c > 0] <- 1
131   diff_m$times2d[diff_m$times2d < 0] <- 0
      diff_m$times2d[diff_m$times2d > 0] <- 1
133   diff_m$times2e[diff_m$times2e < 0] <- 0
      diff_m$times2e[diff_m$times2e > 0] <- 1
135   diff_m$times2f[diff_m$times2f < 0] <- 0
      diff_m$times2f[diff_m$times2f > 0] <- 1
137   diff_m$times2g[diff_m$times2g < 0] <- 0
      diff_m$times2g[diff_m$times2g > 0] <- 1
139   QC_mtimes <- mtimes
      QC_mtimes$times2a <- as.numeric(as.character(QC_mtimes$times2a))
141   QC_mtimes$times2a <- QC_mtimes$times2a * as.numeric(as.character(diff_
        m$times2a))
      QC_mtimes$times2b <- as.numeric(as.character(QC_mtimes$times2b))
143   QC_mtimes$times2b <- QC_mtimes$times2b * as.numeric(as.character(diff_
        m$times2b))
      QC_mtimes$times2c <- as.numeric(as.character(QC_mtimes$times2c))
145   QC_mtimes$times2c <- QC_mtimes$times2c * as.numeric(as.character(diff_
        m$times2c))
      QC_mtimes$times2d <- as.numeric(as.character(QC_mtimes$times2d))
147   QC_mtimes$times2d <- QC_mtimes$times2d * as.numeric(as.character(diff_
        m$times2d))
      QC_mtimes$times2e <- as.numeric(as.character(QC_mtimes$times2e))
149   QC_mtimes$times2e <- QC_mtimes$times2e * as.numeric(as.character(diff_
        m$times2e))
```

```r
    QC_mtimes$times2f <- as.numeric(as.character(QC_mtimes$times2f))
151 QC_mtimes$times2f <- QC_mtimes$times2f * as.numeric(as.character(diff_
    m$times2f))
    QC_mtimes$times2g <- as.numeric(as.character(QC_mtimes$times2g))
153 QC_mtimes$times2g <- QC_mtimes$times2g * as.numeric(as.character(diff_
    m$times2g))

155 writeQCmtimes <- paste("C:\\Users\\mvirdi\\Documents\\Work\\
    ExcelAnalysisVadose\\WaterTable5m\\",AnalysisFolder,"\\times\\", "
    QCmtimes_",KsFactorFile, "Ks.csv",sep="")
    if (RE_WRITE_FILES ==1 )
157   write.csv(QC_mtimes, file = writeQCmtimes, row.names = FALSE)

159 #Calculate R'
    #sets with td for each event #td = temporal diffs | td_theta2a
161 td_sets <- c(paste("td_theta1"),paste("td_theta2",letters[1:set2rains
    ],sep=""))
    for (i in 1: length(sets)) {
163   assign(td_sets[i],eval(as.name(del_theta[i])) )
    }
165 sub_rch_sets <- c(paste("sub_rch_",letters[1:set2rains],sep=""))
    #excess moisture (first 4 m)
167 t <- td_theta2a[,1]
    for (i in 2: length(sets)) {
169   eQ_1m <- 10*( eval(as.name(td_sets[i]))[,2]/2 + eval(as.name(td_sets
    [i]))[,12]/2 + rowSums(eval(as.name(td_sets[i]))[,3:11]) )
    eQ_2m <- 10*( eval(as.name(td_sets[i]))[,2]/2 + eval(as.name(td_sets
    [i]))[,22]/2 + rowSums(eval(as.name(td_sets[i]))[,3:21]) )
171   eQ_3m <- 10*( eval(as.name(td_sets[i]))[,2]/2 + eval(as.name(td_sets
    [i]))[,32]/2 + rowSums(eval(as.name(td_sets[i]))[,3:31]) )
    eQ_4m <- 10*( eval(as.name(td_sets[i]))[,2]/2 + eval(as.name(td_sets
    [i]))[,42]/2 + rowSums(eval(as.name(td_sets[i]))[,3:41]) )
173
    eQ_05m <- 10*( eval(as.name(td_sets[i]))[,2]/2 + eval(as.name(td_
    sets[i]))[,7]/2 + rowSums(eval(as.name(td_sets[i]))[,3:6]) )
175   eQ_15m <- 10*( eval(as.name(td_sets[i]))[,2]/2 + eval(as.name(td_
    sets[i]))[,17]/2 + rowSums(eval(as.name(td_sets[i]))[,3:16]) )
    eQ_25m <- 10*( eval(as.name(td_sets[i]))[,2]/2 + eval(as.name(td_
    sets[i]))[,27]/2 + rowSums(eval(as.name(td_sets[i]))[,3:26]) )
177   eQ_35m <- 10*( eval(as.name(td_sets[i]))[,2]/2 + eval(as.name(td_
    sets[i]))[,37]/2 + rowSums(eval(as.name(td_sets[i]))[,3:36]) )

179   ta_1m <- QC_mtimes[2,i]
    ta_2m <- QC_mtimes[4,i]
181   ta_3m <- QC_mtimes[6,i]
    ta_4m <- QC_mtimes[8,i]
183
```

```r
          ta_05m <- QC_mtimes[1,i]
185       ta_15m <- QC_mtimes[3,i]
          ta_25m <- QC_mtimes[5,i]
187       ta_35m <- QC_mtimes[7,i]

189   # Calculate Normalized Time
          tr_1m <- t/ta_1m
191       tr_2m <- t/ta_2m
          tr_3m <- t/ta_3m
193       tr_4m <- t/ta_4m

195       tr_05m <- t/ta_05m
          tr_15m <- t/ta_15m
197       tr_25m <- t/ta_25m
          tr_35m <- t/ta_35m
199
          pulse_vol <- Ks*SetsFactors[i,PulseFactorColumn]*60
201
          eR_1m <- (pulse_vol-eQ_1m)/pulse_vol
203       eR_2m <- (pulse_vol-eQ_2m)/pulse_vol
          eR_3m <- (pulse_vol-eQ_3m)/pulse_vol
205       eR_4m <- (pulse_vol-eQ_4m)/pulse_vol

207       eR_05m <- (pulse_vol-eQ_05m)/pulse_vol
          eR_15m <- (pulse_vol-eQ_15m)/pulse_vol
209       eR_25m <- (pulse_vol-eQ_25m)/pulse_vol
          eR_35m <- (pulse_vol-eQ_35m)/pulse_vol
211
          rch <- data.frame(tr_05m,eR_05m,
213                         tr_1m,eR_1m,
                            tr_15m,eR_15m,
215                         tr_2m,eR_2m,
                            tr_25m,eR_25m,
217                         tr_3m,eR_3m,
                            tr_35m,eR_35m,
219                         tr_4m,eR_4m)

221       t_05m <- rch$tr_05m[which(rch$tr_05m >= 1 & rch$tr_05m <= t_ratio_
      max)]
          r_05m <- rch$eR_05m[which(rch$tr_05m >= 1 & rch$tr_05m <= t_ratio_
      max)]
223
          t_1m <- rch$tr_1m[which(rch$tr_1m >= 1 & rch$tr_1m <= t_ratio_max)]
225       r_1m <- rch$eR_1m[which(rch$tr_1m >= 1 & rch$tr_1m <= t_ratio_max)]

227       t_15m <- rch$tr_15m[which(rch$tr_15m >= 1 & rch$tr_15m <= t_ratio_
      max)]
```

```
           r_15m <- rch$eR_15m[which(rch$tr_15m >= 1 & rch$tr_15m <= t_ratio_
       max)]
229
           t_2m <- rch$tr_2m[which(rch$tr_2m >= 1 & rch$tr_2m <= t_ratio_max)]
231        r_2m <- rch$eR_2m[which(rch$tr_2m >= 1 & rch$tr_2m <= t_ratio_max)]

233        t_25m <- rch$tr_25m[which(rch$tr_25m >= 1 & rch$tr_25m <= t_ratio_
       max)]
           r_25m <- rch$eR_25m[which(rch$tr_25m >= 1 & rch$tr_25m <= t_ratio_
       max)]
235
           t_3m <- rch$tr_3m[which(rch$tr_3m >= 1 & rch$tr_3m <= t_ratio_max)]
237        r_3m <- rch$eR_3m[which(rch$tr_3m >= 1 & rch$tr_3m <= t_ratio_max)]

239        t_35m <- rch$tr_35m[which(rch$tr_35m >= 1 & rch$tr_35m <= t_ratio_
       max)]
           r_35m <- rch$eR_35m[which(rch$tr_35m >= 1 & rch$tr_35m <= t_ratio_
       max)]
241
           t_4m <- rch$tr_4m[which(rch$tr_4m >= 1 & rch$tr_4m <= t_ratio_max)]
243        r_4m <- rch$eR_4m[which(rch$tr_4m >= 1 & rch$tr_4m <= t_ratio_max)]

245      assign( sub_rch_sets[i-1], makePaddedDataFrame(list(t_05m, r_05m,
                                                              t_1m, r_1m,
247                                                           t_15m, r_15m,
                                                              t_2m, r_2m,
249                                                           t_25m, r_25m,
                                                              t_3m, r_3m,
251                                                           t_35m, r_35m,
                                                              t_4m, r_4m)) )
253
         header <- c( paste("t_0.5m_",letters[i-1],sep=""),paste("r_0.5m_",
       letters[i-1],sep=""),
255                    paste("t_1m_",letters[i-1],sep=""),paste("r_1m_",
       letters[i-1],sep=""),
                       paste("t_1.5m_",letters[i-1],sep=""),paste("r_1.5m_",
       letters[i-1],sep=""),
257                    paste("t_2m_",letters[i-1],sep=""),paste("r_2m_",
       letters[i-1],sep=""),
                       paste("t_2.5m_",letters[i-1],sep=""),paste("r_2.5m_",
       letters[i-1],sep=""),
259                    paste("t_3m_",letters[i-1],sep=""),paste("r_3m_",
       letters[i-1],sep=""),
                       paste("t_3.5m_",letters[i-1],sep=""),paste("r_3.5m_",
       letters[i-1],sep=""),
261                    paste("t_4m_",letters[i-1],sep=""),paste("r_4m_",
       letters[i-1],sep="") )
```

Appendix D (continued)

```
263      colnames(rch) <- header

265      sub_rch_file <- paste("C:\\Users\\mvirdi\\Documents\\Work\\
         ExcelAnalysisVadose\\WaterTable5m\\",AnalysisFolder,"\\rch\\", "rch_
         ",LETTERS[i-1],"_",KsFactorFile,"Ks.csv",sep="")

267      if (RE_WRITE_FILES ==1 )
            write.table(eval(as.name(sub_rch_sets[i-1])), file = sub_rch_file,
          col.names=header, sep=",", row.names = FALSE)
269
      } # End: calculation of Normalised Reacharge-Time for all EVENTS
271
      # Fit Power relation: R' vs. t'
273      events <- LETTERS[1:set2rains]
      names.header <- c("events", paste(seq(1,length(RechargeDepths),1),"m",
        sep=""))
275      filler <- seq(1,7,1)
      powers <- data.frame(paste("Event ", LETTERS[1:set2rains],sep=""),
        filler, filler, filler, filler, filler, filler, filler )
277      colnames(powers) <- names.header

279      for (fit_rain in 1:set2rains) {
        for (fit_depth in 1:length(RechargeDepths)) {
281          x_fit <- eval(as.name(sub_rch_sets[fit_rain]))[-1,fit_depth*2-1]
            y_fit <- eval(as.name(sub_rch_sets[fit_rain]))[-1,fit_depth*2]
283
            if(all(is.na(x_fit))) {
285            powers[fit_rain,fit_depth+1] <- 0
              superpowers[(Ks.this-1)*set2rains+fit_rain,superpowers_misc_cols
        +fit_depth] <- 0
287          }
            else {
289            fit.lm <- nlsLM( y_fit~(1-1/x_fit^p), start = list(p=0.1) ,
        lower = c(0.01), upper = c(7) )
              cfs <- coef(fit.lm)
291            powers[fit_rain,fit_depth+1] <- cfs[1]
              superpowers[(Ks.this-1)*set2rains+fit_rain,superpowers_misc_cols
        +fit_depth] <- cfs[1]
293          }
         }
295
         powers_file <- paste("C:\\Users\\mvirdi\\Documents\\Work\\
        ExcelAnalysisVadose\\WaterTable5m\\",AnalysisFolder,"\\powers\\", "
        Powers_",KsFactorFile,"Ks.csv",sep="")
297      if (RE_WRITE_FILES ==1 )
            write.csv(powers, file = powers_file, row.names = FALSE)
```

84

```
299   } # End: 'power−fitting' for this Ks.this
    } # End: Loop over all Ks
301
    superpowers_file <− paste("C:\\Users\\mvirdi\\Documents\\Work\\
        ExcelAnalysisVadose\\WaterTable5m\\",AnalysisFolder,"\\", "All_
        SuperPowers",".csv",sep="")
303 if (RE_WRITE_FILES ==1 )
        write.csv(superpowers, file = superpowers_file , row.names = FALSE)
```

ProcessHYDRUS_1D.R

About the Author

Makhan Virdi received his Bachelor of Technology (B.Tech.) in Civil Engineering from the Indian Institute of Technology (IIT Roorkee, India) in 2004. In 2005, he moved to the USA to pursue graduate studies at the University of South Florida (Tampa). He graduated with a Masters in Civil Engineering in 2008. While at USF, he worked for the U.S. Geological Survey from 2007 to 2010 studying surface-groundwater interactions by modeling long-term climatic effects on a karst lake. His research interests include Geospatial analysis, Time-series analysis, Hydrological modeling, Variably-saturated flow modeling, and Numerical simulations. After completion of his Ph.D., he is going to work as a postdoctoral researcher in biogeochemical dynamics in one of NASA's Earth Observing System Data and Information System (EOSDIS) data centers at the Oak Ridge National Laboratory.

Apart from academic research, Makhan is involved in various development projects at *InfinityXLabs*. These projects combine components from computer programming, electronic sensors, hardware programming, amateur (*ham*) radio, semantic knowledge base, and robotics. He is interested in the fusion of these interdisciplinary projects into *machine augmented intelligence* systems.

"La semplicità è l'ultima sofisticazione"

[Simplicity is the ultimate sophistication]

– Leonardo da Vinci